Critical Regulators of Epithelial Homeostasis and Intestinal Crypt Regeneration: Identification of Novel BVES/BCAR3 Signaling Complex in EMT and Tumorigenesis and Biological Implications for MTG16 in Stem Cell Function, Proliferation, Apoptosis and DNA Repair.

By

Shenika Vonsha Poindexter

Dissertation

Submitted to the Faculty of the

Graduate School of Vanderbilt University

In partial fulfillment of the requirements

for the degree of

DOCTOR OF PHILOSOPHY

In

Cancer Biology

May 2015

Nashville, Tennessee

Approved:

David Bader, Ph.D.

Linda Sealy, Ph.D.

Christopher Williams, M.D., Ph.D.

Albert Reynolds, Ph.D.

DEDICATION

I dedicate this thesis to my family, especially my mother who has been my pillar of strength during the highs and lows of graduate school.

ACKNOWLEDGEMENTS

This work would not have been possible without the financial support of the of the Vanderbilt GI SPORE Career Development Award, Vanderbilt DDRC Pilot Award and the VA Merit, and T32 CURE Supplement Training Grant. Many people have contributed to my growth and personal development throughout my time as a graduate student. I am grateful for Dr. Roger Chalkley and Dr. Linda Sealy for their support, advice and recommendations throughout my graduate studies. They have helped me overcome many obstacles during my academic career and have been a huge source of inspiration, information, and motivation. Drs. Chalkley and Sealy played a critical role in helping me identify an awesome research supervisor, who would later become one of my greatest mentors.

I would like to express my appreciation to Dr. Christopher Williams, my research supervisor, for taking the time to provide guidance, support and advice throughout the years. As my supervisor and mentor, Dr. Williams has shown me what it takes to be a good scientist and overall good person. I am very grateful for his time, patience, and willingness to help with both academic and personal challenges. During my time the Williams' lab, I have learned essential life skills. Perhaps, the most important lessons include understanding different perspectives and being open to constructive criticism. I am confident that these skills will contribute to both my professional and personal life. It has truly been a pleasure working with Dr. Williams.

Thank you to the members of the Williams' Lab. We have shared so many great times and I will forever cherish the memories. I am grateful for every

presentation, and article that they have helped me to refine. I appreciated the time shared during conferences and lab outings. I felt that everyone contributed to my growth not only a scientist but as a person. I wish them all the best in their future endeavors and I look forward to hearing of future success. It has truly been a pleasure working with everyone and I am very sad to leave such a wonderful group. Their support and encouragement along the way has been invaluable.

Special thanks to collaborators and colleagues for their time and energy, intellectual discussions, and constructive feedback on papers, experiments, and projects and etc. I would not have made any progress without their contributions.

I am very grateful to the members of the dissertation committee for the constructive suggestions, patience, and sharing a wealth of knowledge and experience.

In closing, I would be remiss if I did not acknowledge my family and friends. I could not have completed my dissertation without their unconditional love and support. I am so grateful for their encouraging words and prayers throughout my studies. Graduate school is challenging and there were times that I didn't think I would make it. Because of my support system, I continued to push through and for that I am forever grateful.

TABLE OF CONTENTS

Page

LIST OF FIGURES

Chapter I. Introduction

Biology of the Intestine

The gastrointestinal (GI) tract is primarily responsible for the digestion and absorption of nutrients [1], [2]. The intestine is a muscular hollow organ that extends from the pyloric sphincter of the stomach to the anus [2]. It is divided into the upper and lower GI tract [1]. The upper GI tract consists of the mouth, esophagus, and stomach [1], [3]. The lower portion consists of the small and large intestine [1], [4].

The large intestine consists of four parts: the cecum, colon, rectum and anal canal [5]. The cecum is the pouch-like structure that connects the small intestine to the large intestine [2], [5]. The colon makes up most of the large intestine and can be divided into 4 sections: the ascending colon, the transverse colon, the descending colon and the sigmoid colon [5]. The terminal portion is the sigmoid colon that descends to form the rectum and anal canal [1], [2], [5] . Functionally, the large intestine primarily secretes mucus, a substance that serves to lubricate and protect the mucosa from mechanical and chemical injury [2].

The mucosa, by definition, is a protective barrier that separates the body's external environment from the internal milieu [6]. The mucosal barrier consists of 4 layers -the mucosa, sub mucosa, muscularis externa and serosa [1], [2], [4]. The mucosa is the innermost layer that surrounds the open tube-like cavity known as the lumen [2]. The mucosal layer consists of the epithelium, lamina propria, and muscularis mucosae [2]. The epithelium is the innermost layer and is surrounded by a layer of connective tissue lamina propria; the muscularis mucosa is the

outermost layer of the mucosa; the sub mucosa lies between the mucosa and the muscularis externa [2], [4], [7]. The sub mucosa is comprised of connective tissue, lymphatic vessels and large blood vessels and nerves that branch into mucosa and the muscularis externa, a circular layer and a longitudinal outer muscular layer [2], [4]. Finally, the serosa is the outermost layer of the mucosal barrier and it is made of dense connective tissue [2].

The small intestine is where most digestion and absorption take place [1], [2], [4]. It is divided into three segments: the duodenum (2.5 cm), the jejunum (2.5 m) and the ileum (3.6 m). The duodenum receives the food from the stomach and neutralizes it [4]. The jejunum or midsection of the gut is comprised of circular folds and fingerlike projection known as villi [1], [2]. The villi are responsible for increasing the surface area; each villus is lined by simple columnar epithelial cells and comprised of a connective tissue core, a capillary network, and a central lacteal or terminal lymphatic vessel [1], [2], [7]. Between the villi are the shallow invaginations known as crypts of Lieberkűhn, lined with epithelial cells [2].

The turnover time of the crypt-villus unit is 3-5 days, making it the fastest self-renewing tissue in mammals [8]. During the intestinal self-renewal process, stem cells that reside at the base of the crypt give rise to transit amplifying (TA) cells [8]. The TA cells migrate up the crypt-villus axis and differentiate into absorptive cells (enterocytes) or secretory lineages (enteroendocrine, goblet, or Paneth cells). The enterocytes contain microvilli that increase surface area for absorption and cells that commit to the secretory lineage serve to that secrete mucus or anti-microbial to protect the lumen. After lineage commitment, these cells

migrate up the crypt-villus axis to help the villi push off the older cells at the tips of the villi, a process denoted as sloughing and shed into the lumen [8]–[10] (Figure 1). Due to the rapid cell turnover, intestinal crypt cells are sensitive to radiation and anticancer drugs that block mitosis [11]–[13].

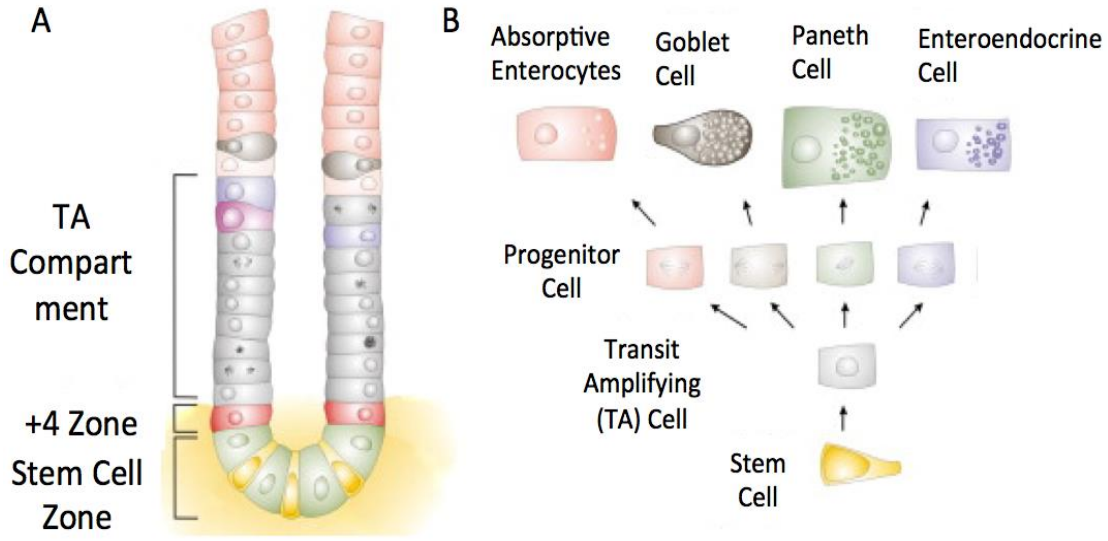

Figure 1. Adult Stem Cell-Driven Epithelial Renewal in the Small Intestine. (A)The general architecture of a crypt. (B) Flowchart depicting generation of functional epithelial cells from an intestinal stem cell [142]

Development of Colon Cancer

Vogelstein and Fearon described the first genetic model of colorectal cancer as the accumulation of acquired genetic and epigenetic events that transform the normal epithelium to adenocarcinoma [14]. One of the first histological lesions to be observed is the aberrant crypt foci (ACF) [15]–[17]. ACF presents as enlarged slightly elevated lesions on the mucosal surface and typically harbor mutations in Adenomatous Polyposis Coli (APC) (Figure 2). As the ACF progresses to a polyp and eventually a carcinoma, it acquires mutations in the tumor suppressor, TP53

(Figure 2). Notably, APC is one of the most commonly mutated in hereditary colorectal cancers such as familial adenomatous polyposis (FAP) and hereditary nonpolyposis colorectal carcinoma (HNPCC) or lynch syndrome. .

Mechanistically, the APC protein forms a complex with B-catenin to stimulate its degradation in normal cells [18]. However, in colorectal cancer, APC

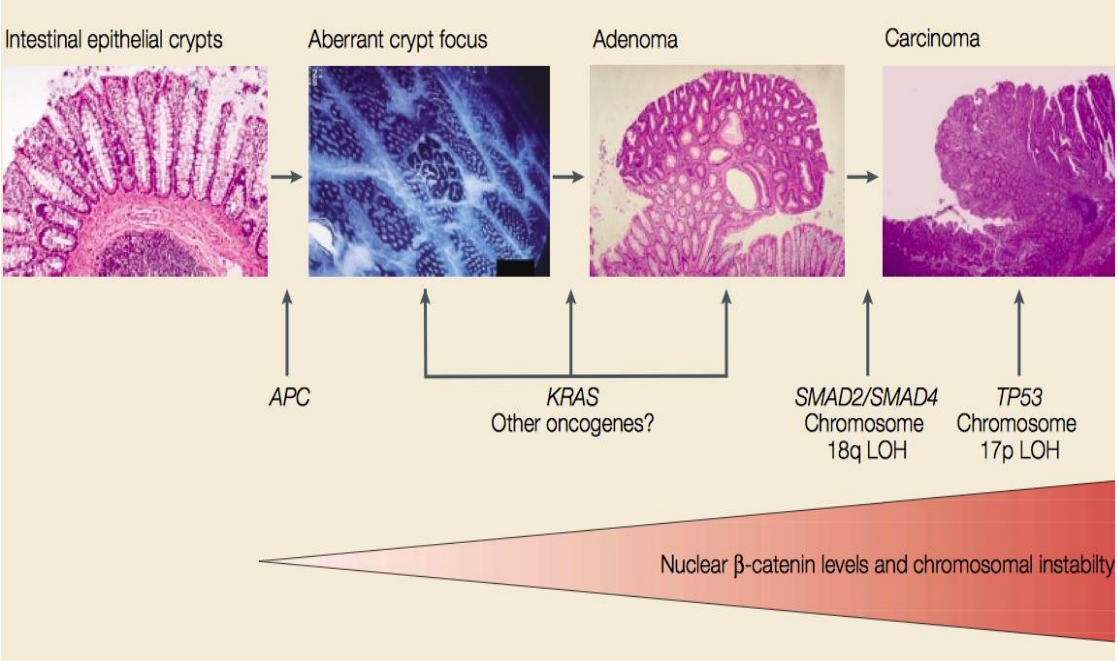

Figure 2. Histopathology of Colorectal Cancer. A, H&E staining of colonic epithelium B, Methylene blue staining of colorectal neoplastic showing Aberrant Crypt Foci (ACF). C, ACF usually encompass few crypts and can be composed either of cells of normal morphology (nondysplastic), or dysplastic cells. The latter are more likely to progress to become a polyp. (C) H&E staining of a benign tumor mass that protrudes into the lumen from the intestinal epithelium. Polyps, like their ACF counterparts, can be of two types: hyperplastic (nondysplastic) and adenomatous (dysplastic). Hyperplastic polyps preserve normal architecture and cellular morphology (D) H&E staining of adenomatous polyps that are characterized by abnormalities in both inter- and intracellular organization. The epithelium is organized in multiple layers, nuclei are enlarged, and their alignment at the basal membrane is lost [18].

mutations stabilize β-catenin in the cytoplasm; free cytoplasmic β-catenin translocates to the nucleus to bind to T Cell Factor 4 (TCF4) to promote transcription of the Wnt target genes and subsequent hyperproliferation [19]–[21].

In addition to regulating the WNT signaling pathway, APC has been implicated in cell adhesion signaling pathways [22]–[24]. In colorectal tumors, APC plasma membrane association is lost [25]. Other roles for APC include binding actin and actin-associated proteins [26]. However it is unclear whether APC association is responsible for regulating the latter.

Tight Junctions

In addition to mutations in APC, mutations in adherens junctions (AJs) and tight junctions (TJs), have been linked to tumorigenesis [27], [28]. AJ's are composed of E-cadherin, a single transmembrane protein. TJ's are composed of occludins and claudins, which are tetra-spanin proteins [29]. AJ's and TJ's are important regulators of cell adhesion, polarity, and proliferation. In normal epithelia, TJs have two main functions: (1) divide the epithelium into apical and basolateral domains to prevent the mixing of substances and (2) to prevent the passage of macromolecules such as ions and solutes between cells. Zonula Occludens (ZO) proteins have been demonstrated to link TJs to the actin cytoskeleton [29], [30]. In tumors, TJ integrity is often compromised with Claudin-1 and ZO-1 mislocalized to the nucleus and E-cadherin underexpressed via promoter methylation [30]–[32]. Specifically, Claudin-1, -3, -4, and -7 overexpression has been implicated in ovarian, CRC, and gastric cancers [32],[33], [34]. E-cadherin loss contributes to increased levels of cytoplasmic β-catenin. Free β-catenin translocates to the nucleus and promotes transcription of genes responsible for proliferation and survival [23], [35]. In summary, disruption and mislocalization of AJ and TJ

dysfunction have been linked to protumorigenic signaling pathways including regulation of WNT signaling and RhoA signaling [27], [28], [32].

Epithelial Mesenchymal Transition (EMT)

Colon cancer cells acquire mesenchymal traits including changes in cell morphology, loss of junctional adhesion markers such as E-cadherin, ZO-1,

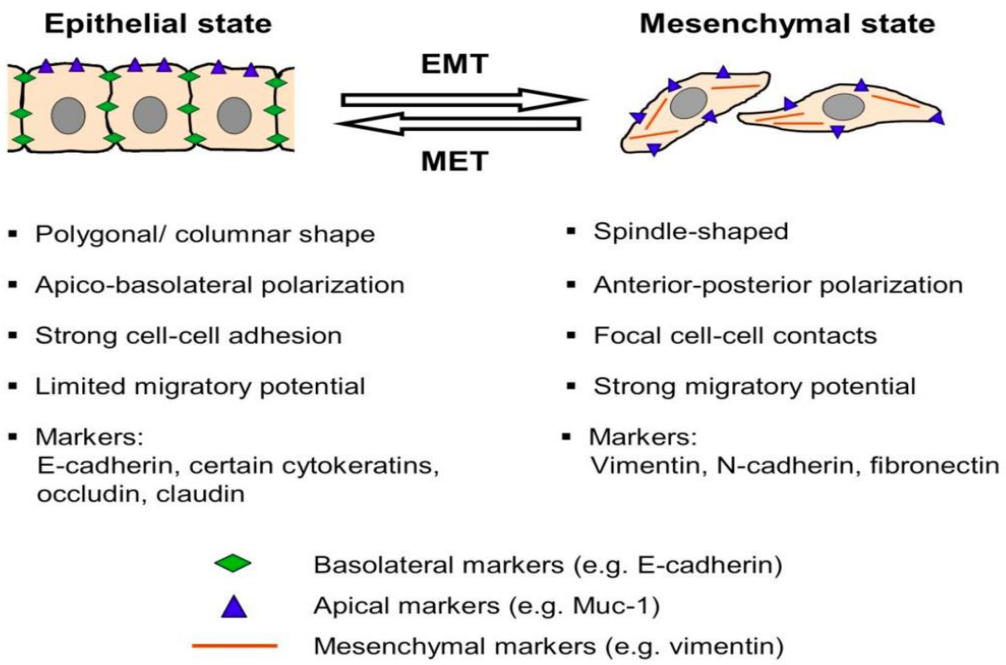

Figure 3. Characteristics of Epithelial Mesenchymal Transition (EMT) and Mesenchymal Epithelial Transition (MET) [143]**.**

expression of mesenchymal markers including vimentin, N-cadherin and undergo increased migration and proliferation [36], [37]. The aforementioned processes are characteristic of epithelial to mesenchymal transition (EMT) (Figure 3).

Blood Vessel Epicardial Substance

Blood Vessel Epicardial Substance (BVES), a cell adhesion molecule that is downregulated in colon cancer [38], was originally discovered in a screen to identify genes involved in coronary blood vessel development [39]. Although BVES

has no recognizable structural domains that would suggest a function, it is highly conserved across species with the highest degree of homology in its C-terminus [40]. BVES has been demonstrated to be 338 amino acids (a.a.) in frog, 357 a.a in chicken, 358 a.a. in mouse, and 360 a.a. in human and is known to be expressed in muscle tissues including striated and smooth muscle cells and epithelial tissues, including eye, gut, and respiratory epithelium [41]–[43]. Structurally, BVES has an extracellular N-terminal domain, three transmembrane domains, and an intracellular C-terminal domain [44] (See Chapter 2: Figure 7). There are two N-glycosylation sites within the N-terminal region. The C-terminal region contains a Popeye domain [44]. BVES detection in the absence and presence of a reducing agent reveals a series of bands that range from 41 to 58-kDa respectively. The differences in molecular weight may be due to the N-terminal N-glycosylation sites or alternative splicing events [45]. BVES is one of the three Popeye domain containing (Popdc) family members. The other two family members, Popdc2 and Popdc3, are also conserved across species [41], [46]. Closer examination reveals a 50% sequence homology between BVES (Popdc1) and Popdc2 and 25% homology between Popdc2 and Popdc3 [41], [46], [47]. BVES and Popdc3 are located on the same chromosome suggesting that there is a redundant function. Whereas, Popdc2 is on a different chromosome suggesting that its function may be different from the other two family members [46]. BVES is able to homodimerize and heterodimerize with other Popeye family members [44], [45], [48]. In vivo studies report that BVES knockout mice exhibit no overt phenotypes but present with delayed musculoskeletal regeneration after cardiotoxin injury [42].

BVES Regulates EMT and MET Balance

Determining expression pattern for BVES is critical to understanding BVES function. During chick embryogenesis and epithelial generation of the eye, BVES is localized to the apical-lateral areas [40], [49]. During coronary development BVES cannot be detected at the surface of the cells and as a result, the epithelial cells become more mesenchymal-like [50]. BVES colocalizes with adherens and tight junction markers, E-cadherin and ZO-1 [40], [49]. When cells are polarized or have formed an epithelial sheet, BVES is almost completely localized to the cell membrane and cannot be detected intracellularly [49]. In human corneal epithelial cells (HCECs), it appears that BVES membrane expression is lost during migration but after cells establish contact, BVES expression is restored [49], [51].

Using reverse genetic approaches, studies have reported that epithelial cells acquire mesenchymal like features upon silencing BVES expression. For example, knockdown of BVES expression in HCEC's result in faster migration, loss of epithelial integrity, and decreased expression of adhesion molecules [49]. Additional studies using a Xenopus model report that silencing BVES expression disrupted organogenesis and disorganized migration during embryogenesis [52]. Further studies using a Drosophila model, implicated a role for BVES in photoreceptor cellular polarity, a process that has been cited to be relatively similar to epithelial cell polarity [53]. In L-Cells, a non-adherent cell line, BVES expression promotes cell aggregation [54]. Lastly, overexpression studies using a BVES N-terminal truncation mutant or full-length BVES construct in NIH 3T3 fibroblasts increases cell roundness and decreases migration, respectively [24], [40].

Through the use of BVES mutants, Kawaguchi and colleagues demonstrated that mutation of Lysine 272 and 273 (BVES KK mutant) in the BVES C-terminal domain are required for BVES-BVES homodimerization [51]. Functionally, expression of BVES KK mutant decreased cell aggregation in L-Cells and caused mislocalization adhesion proteins and decreased trans-epithelial resistance (TER) in HCEC's [48].

BVES Interactions

BVES has a popeye domain but no other identifiable motifs. Because of this, understanding BVES-protein interaction networks might provide insight into BVES function. Bader and colleagues performed a yeast 2-hybrid screen and identified guanine nucleotide exchange factor T (GEFT), a GEF that regulates rho family small GTPases- Cdc42 and Rac1 [24], as a BVES interacting protein. GEFs are responsible for cycling of GTPase from the GDP-bound (inactive) to the GTP bound (active) state [55]. Following Rho GTPase activation, a cascade of downstream signaling events are initiated including cell adhesion, movement, proliferation, and microtubule cytoskeleton reorganization. Rho GTPases are also critical for maintenance of the epithelial barrier [56]. Activation of Rac1 promotes membrane ruffling and lamellipodia extension and activation of Cdc42 initiates filopodia formation [57]. Interestingly, BVES expression in Cdc42, Rac1 expressing NIH3T3 cells promotes cell roundness, decreases cell movement and decreases Rac1 and Cdc42 activity [56]. Based on these results, BVES might interact with GEFT to influence Rho GTPase activity.

Additional studies from Bader and collegues demonstrate that BVES interacts with Vesical Asscoiated Membrane Protein 3 (VAMP3), a SNARE protein that facilitates

vesicular transport and recycling of integrins. Specifically, VAMP-3, is important for the transport and recycling of transferrin and β-1-integrin [52]. Disruption of VAMP3 in normal cells, results in decreased cell adhesion and BVES interaction with Vamp3 might explain the previously observed adhesion and migration phenotypes.

BVES regulates cellular proliferation through an interaction with Zonula Occludens 1-associated Nucleic Acid-Binding protein/DNA-binding protein A (ZONAB/DbpA), a y-box transcription factor that is recruited to tight junctions [58]. ZONAB regulates transcriptional activity of cyclin D1, a known regulator of cell cycle [58]. When ZONAB is bound to tight junctions its function is suppressed and cell proliferation is inhibited. Most recently, the ZONAB/GEFH1 interaction has been demonstrated to be critical for cyclin D1 promoter activation [59]. Thus, the BVES/ZONAB interaction could be one mechanism by which BVES may indirectly interact with GEFH1 to mediate its effects on cell proliferation. Collectively, these studies highlight roles for BVES in cell adhesion, morphology, migration and Rho signaling- all of which are important in EMT or MET processes.

BVES in Colon Cancer

BVES is mislocalized in colorectal cancer (CRC) patient tissue samples [38]. Immunofluorescence (IF) for BVES demonstrates that BVES is localized at the apical domain of colonocytes. In contrast, tumor tissue revealed both disorganized BVES localization and significantly reduced expression. Data from a cDNA array revealed BVES expression is silenced at all stages of CRC and even at an earlier adenoma stage when compared to the normal mucosa. Expression array also revealed that BVES expression is not only decreased in the colon but the breast tumor tissue as well. As mentioned previously, Popdc1/BVES has two

other family members: Popdc2 and Popdc3. BVES and Popdc3 expression were down regulated in a panel of CRC cell lines as compared to Young Adult Mouse Colonic (YAMC) control cells, a “normal” epithelial cell line. Interestingly, Popdc2 expression was unaffected in this panel of CRC cell lines. One possible explanation for the differences is that Popdc1/BVES and Popdc3 are located on the same chromosome and this might suggest that function is regulated by a similar mechanism. BVES expression in LIM2405 cells decreased expression of mesenchymal marker, vimentin and increased expression of epithelial marker E-cadherin, ZO-1 and Occludin-1 (Figure 4). Additionally, BVES expression in LIM2405 cell lines decreased migration, invasion, TER, and anchorage independent growth (Figure 4).

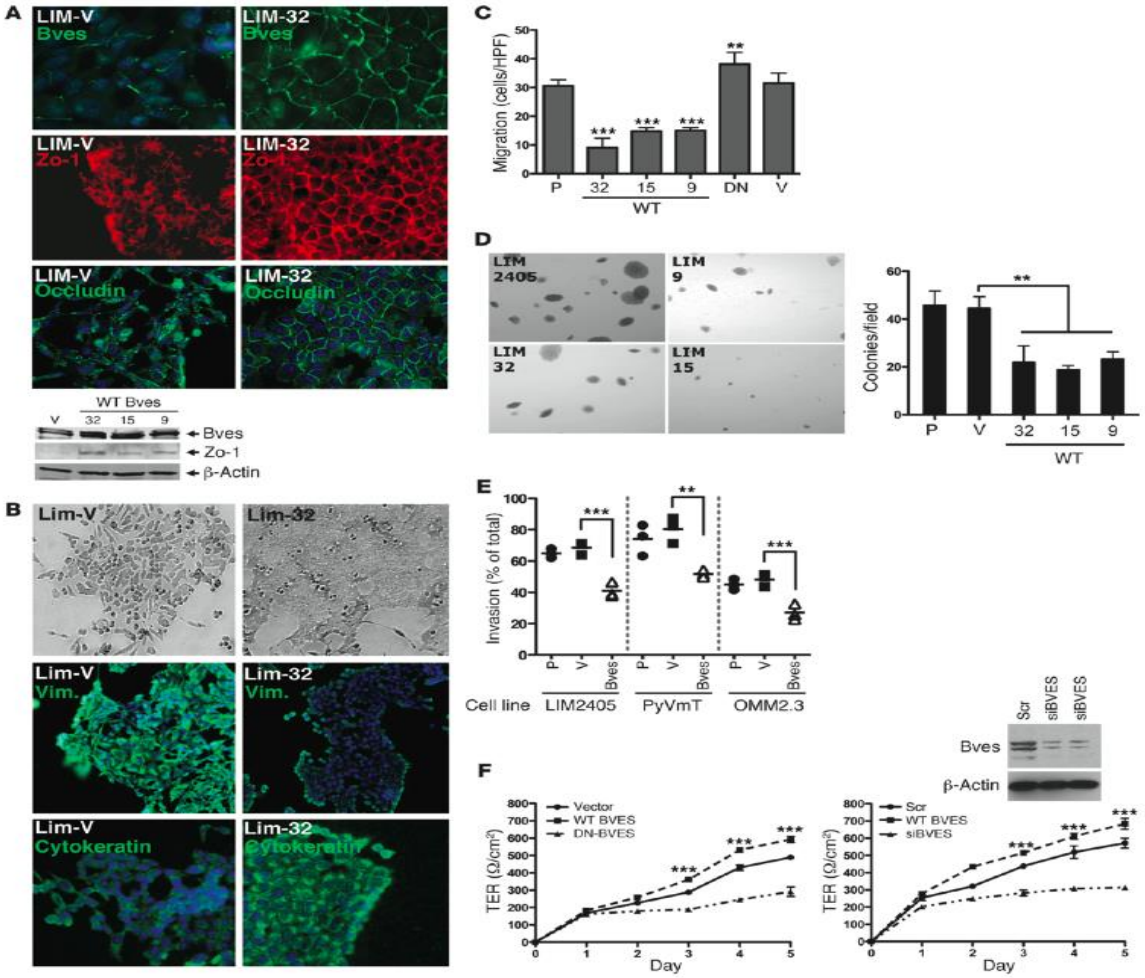

Figure 4. BVES induces an epithelial-like phenotype in carcinoma cells. A, Immunofluorescent microscopy for BVES, ZO-1, and Occludin in LIM2405-V (LIM-V) or LIM2405 BVES-expressing (LIM-32) cells. DAPI stain (blue) was used to identify nuclei. Western blot analysis of BVES and ZO-1 protein levels in LIM2405-V cells or 3 independent BVES-expressing clones (LIM-32, LIM-15, and LIM-9, referred to as 32, 15, and 9, respectively) (original magnification, ×200). B, Phase-contrast microscopy and immunofluorescent staining for the vimentin (Vim.) and cytokeratin (original magnification, ×200). C, Wound healing assay. LIM2405-P (P), LIM2405-V (V), LIM2405-BVES clones (32,15,9), and LIM2405 cells stably expressing a carboxy terminal deletion BVES construct functioning as a dominant negative (DN) were used. Data is represented as the mean ± SD. ***P < 0.001, **P < 0.01, Student's t test. D, Anchorage-independent growth assay (original magnification, ×100). Colonies were tallied on day 14. Colony size and colony number are shown. Data are presented as mean ± SD. HPF, high-powered field. **P < 0.01. E, Boyden chamber invasion assay was performed using LIM2405, PyVmT (murine breast carcinoma; ref. 53), or OMM2.3 (ocular melanoma) cells. Individual symbols represent individual cells, and horizontal bars represent the median. **P < 0.01, ***P < 0.001, Student's t test. F, CACO2 cells transiently transfected with the indicated constructs. Upon achieving confluence, trans epithelial resistance was measured daily (n = 6). ***P < 0.001, Student's t test [38].

Knockdown of BVES expression in CACO2, an epithelial cell line, and subsequent implantation of these cells into nude mice resulted in larger tumor burden when compared to mice implanted with control cells. Injection of BVES expressing SW620 cells decreased invasion when compared to mice injected with non-BVES expressing SW620 cells. Migration, invasion, anchorage independent growth and upregulation of epithelial markers are characteristic of Mesenchymal to Epithelial Transition (MET). Taken together these data demonstrate the BVES is critical for regulating the balance between EMT and MET programs.

Mechanistically, BVES has been linked to both WNT and RhoA signaling pathways. Previous studies in our lab demonstrate that silencing BVES expression increased Wnt induced-TopFlash activity. Additionally, co-expression of BVES and GEFT (a BVES binding partner), partially rescues RhoA activity, suggesting that BVES has potential to interact with multiple partners to regulate Rho mediated signaling [60].

To identify other BVES interacting proteins that regulate Rho signaling, we commissioned a Yeast 2-hybrid screen. We identified Breast Cancer Antiestrogen Resistance 3 (BCAR3), a regulator of breast cancer cellular proliferation, Rho Signaling, and anti-estrogen resistance in breast cancer, as a BVES binding partner.

BCAR3 Structure

Breast cancer antiestrogen resistance 3 (BCAR3) was identified in a screen for genes whose expression confers resistance to anti-estrogens [61]. BCAR3 is a 95-kDa protein that belongs to the novel Src homology 2 (SH2)-containing protein

(NSP) family [62], [63]. BCAR3/NSP2, also known as AND34 in mice, has two other homologs, NSP1/BCAR1/p130Cas and NSP3/Chat/SHEP1 [64], [65]. The family shares two common domain structures, SH2 domain and a RAS GEF domain with 30% homology to the CDC25 family of GEFs [65] (Figure 7). BCAR3 carboxyl terminus binds to the carboxyl terminal domain of p130Cas, Crk-associated substrate (Cas), a focal adhesion molecule that contributes to linkage of the cytoskeleton to the extracellular matrix and is crucial for maintenance of cell contact in normal cells [66], [67]. X-ray crystallography studies have confirmed that tight linkage exists between BCAR3 and CAS proteins [68]. Of the NSP family members, BCAR3 is the only NSP family member that induces anti-estrogen resistance [64]. A survey of estrogen receptor positive, mesenchymal, and estrogen receptor negative breast cancer cell lines reveal that BCAR3 expression is highest in estrogen receptor negative, mesenchymal cell lines [64].

BCAR3 Regulates Intracellular Signaling Pathways

BCAR3 contributes to a myriad of signaling pathways important for focal adhesion signaling and EMT. In cancer, focal adhesions disassembly and assembly are central to EMT-mediated processes including migration, invasion and metastasis [67]. BCAR3 knockdown influences EMT by regulating endogenous Cas and c-Src activity in breast cancer cells [69]. BCAR3 loss impacts the Cas/Src signaling axis by decreasing Cas/Src association. c-Src is a nonreceptor tyrosine kinase that that is responsible for many cellular processes, including proliferation, adhesion, migration, and invasion. c-Src is tightly regulated by Cas [70]. c-Src phosphorylates Cas and Cas activates Src, the synergistic activity promotes cell

proliferation and survival (Figure 5) [70]. This interaction has been demonstrated to be due to the binding of BCAR3 to the SH2 domain of BCAR1/p130Cas.

As mentioned before, BCAR3 expression is highest in estrogen receptor negative cell lines. Thus making estrogen receptor negative cell lines an optimal cell line to study BCAR3 function. Learner and colleagues silenced BCAR3 expression in MDA-MB-231, an estrogen receptor negative breast cancer cell line, and demonstrated that loss of BCAR3 prevents p130Cas localization to the membrane and promotes increased cohesiveness and decreased cell projections in breast cancer cells [71]. Makkinjee and colleagues generated a BCAR3-R743A mutant that failed to bind p130Cas and demonstrated that BCAR3 can signal independently of p130Cas; these results suggest that BCAR3 dependent and independent p130Cas signaling pathways promote cell proliferation, cell spreading and adhesion [71], [72].

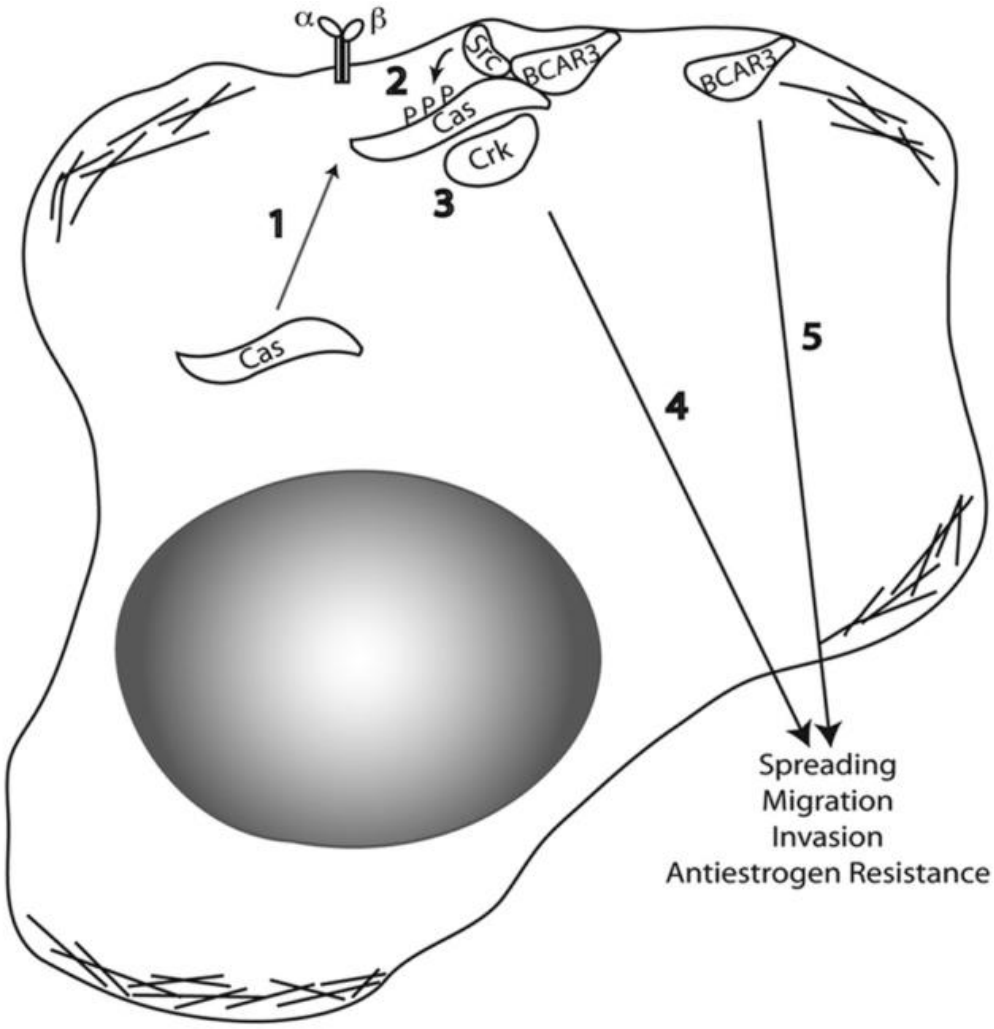

Figure 5. Proposed mechanism of BCAR3-mediated enhancement of c-Src activation, cell spreading, and adhesion. Step 1, cytosollically localized Cas is recruited to membrane-proximal regions by BCAR3 through an indirect or direct interaction with BCAR3. Once at the membrane (step 2), Cas interacts with and activates c-Src. c-Src activation results in the phosphorylation of Cas, which leads to the recruitment of substrate domain binding partners such as Crk (step 3). Step 4, Cas/Crk interactions activate downstream signaling pathways important for cell spreading, migration, and invasion. BCAR3-dependent and BCAR3-independent c-Src signaling can also activate other signaling pathways important for cell proliferation and survival in the presence of antiestrogens. Step 5, BCAR3 itself activates an unidentified c-Src-independent pathway important for cell spreading [69].

Myeloid Translocation Genes in Biology

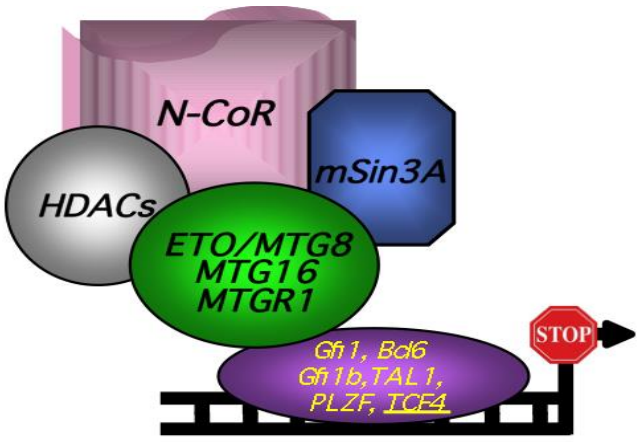

Figure 6. Schematic of the MTG/HDAC/N-CoR/mSin3A Repression Complex.

Myeloid Translocation Genes (MTG's) were discovered in acute myeloid leukemia (AML) [73], [74]. The 8:21 translocation commonly seen in AML results in an in-frame fusion of the DNA binding domain of RUNX1 and the transcriptional repression domain of MTG8. This translocation alters the normal function of the transcription factor RUNX1 and leads to repression of RUNX1 target genes [74]. There are two other MTG family members, MTG16 and Mtgr1. All MTGs form repression complexes with HDACs, N-CoR, and mSin3A to bind transcription factors and shut down transcription (Figure 6) [73]. Since MTG's do not have a DNA binding domain, they do not bind the DNA directly [73], [75], MTGs serve as a scaffold complex that binds to the transcription factors such as T-cell factor 4 (TCF4) to shutdown TCF4 dependent transcriptional programs [76]. TCF4 is a critical regulator for the Wnt signaling pathway, an important player in the stem cell regulatory pathway. Because of MTG's association with TCF dependent stem cell regulatory signaling pathway, it is critical for epithelial homeostasis and is frequently targeted in malignancy [76].

MTGs play a role in several biological processes including stem cell function, malignancy and differentiation. MTG8 knockout mice exhibit deletion of

the midgut leading to perinatal lethality [77]. MTG8 and MTG16 have been implicated in epithelial malignancies, with the identification of multiple nonsynonymous mutations in MTG8 and MTG16 in colorectal carcinoma and more recently, additional mutations in MTG8 identified in breast and lung cancer [78], [79]. We have demonstrated that MTGR1 knockout mice exhibit differentiation defects in the intestine and abnormal response to chemically-induced injury [80].

Most recently, we demonstrated that MTG16 is a critical regulator of colonocyte proliferation and intestinal barrier function [60]. Specifically, MTG16 loss augmented colonocyte proliferation and epithelial permeability; MTG16 loss promoted greater histologic injury and increased *C. rodentium* colonization [60]. Overall, MTG16 loss exacerbated innate and adaptive immune responses after DSS-induced injury while MTG16 mice were protected from DSS-induced injury [60]. Of the MTG family members, MTG16 is most highly expressed in early progenitor stem cell populations [81]. After stress, hematopoietic progenitor cells fail to mature into erythroid cells in *Mtg16*$^{-/-}$ mice [82]. Mechanistically, disruption of MTG16 results in de-repression of DNA binding factors including PLZF, BCL6, TAL, and GFI [82]. Because MTG16 acts as a scaffold for these co-repressors, Mtg16 loss impacts cell fate decisions and commitment to hematopoietic cell lineages [82].

Radiation Enteritis

Radiation enteritis is the term used to describe the inflammatory process that occurs in the intestine following radiation exposure. For patients that have undergone radiotherapy, signs and symptoms include a loss of appetite, nausea

and diarrhea. However, in patients with radiation enteritis these symptoms can persist [69]–[71]. Special diets and medication can help control the symptoms and improve your quality of life. Surgery is occasionally needed. Symptoms of radiation enteritis that occur up to 90 days following treatment are termed acute injury. During this stage there is mucosal injury and inflammation that lead to epithelial barrier disruption. Delayed symptoms that occur months to years after radiotherapy is termed chronic injury and manifest as transmural fibrosis and vascular damage [83], [84]. Additionally, patients receiving radiation for pelvic malignancies concurrent with chemotherapy increases patient risk for developing radiation enteritis [85]. Some of the genetic risk factors associated with radiation enteritis include mutations in DNA repair genes such as *BRCA1* and *BRCA2* and apoptotic genes such as *Tp53* and *BCL6* [86], [87], [88], [89].

Some of the molecular mechanisms that may explain sensitization to intestinal radiation-induced injury include changes in cell cycle kinetics, synchronization of replicating cell populations, and inhibiting effective DNA repair that ultimately result in increasing the amount of radiation-induced DNA damage [88], [90]. One of the most well established pathways involved in radiation-induced DNA damage includes induction of DNA double stranded breaks and recruitment of histone H2A.X and phosphorylation of a number of mediators that phosphorylate Tp53 and triggers apoptosis [91], [92].

Effects of Radiation on Intestinal Stem Cells

The initial apoptosis occurs in the stem cell compartment. One of the molecular players that contributes to damage detection and apoptosis induction is

p53. Peak induction usually occur within a period of 3-6 hours [93]. When there is a low level DNA damage, a rapid response is elicited including accelerated cell cycle and increased self-maintenance probability of neighboring stem cells. Radiosensitivity of some stem cells can be attributed to an “extreme self screening process” that implies that DNA repair is not activated but rather cell suicide is initiated [92], [94], [95].

Crypt Regeneration After Injury

According to the crypt irradiation recovery model, mature cells can de-differentiate to replace lost stem cells not just the TA compartment [10]. In support of this model, Van Landeghem *et al* have shown that Sox9+^{Low} Intestine Epithelial Stem cells and Sox 9+ High Secretory epithelial cells participate in crypt regeneration after radiation injury. The transcriptional networks that drive cell fate toward different secretory cell lineages are activated in the sox9$^{EGFP\ High}$ cells during crypt regeneration [96].

In contrast, in high radioresistance circumstances a certain number of cells in early transit division can be recruited back into the stem cell compartment suggesting there is a highly efficient repair process [95]. Furthermore, the daughter cells are derivatives of normal cells and are unlikely to acquire mutations as a consequence of misrepair. This may serve as a protective mechanism for the small intestines in terms of genetically damaged stem cells and carcinogenic risk [9].

Diagnostics/Cancer Therapy

Since colon cancer is an age related disease and impacts individuals over 50, Colonoscopy is strongly recommended [83], [97], [98]. For patients that have

germline mutations in APC they are at risk for developing polyps earlier and should go for colonoscopy screenings at an earlier time period. Colonoscopy is the gold standard for detecting colonic polyps. Once cancer is diagnosed the patient has to undergo either chemotherapy or surgical resection. Patients receiving radiation for pelvic malignancies concurrent with chemotherapy increases patient risk for developing radiation enteritis [84], [85], [99]. It is not guaranteed that every patient will respond to chemotherapy and even then the patient may suffer from side effects including vomiting, nausea, diarrhea or possibly acute or chronic radiation enteritis [83], [85], [99]. In some cases, colonic resection is recommended. Both procedures are invasive and drastically decrease the patient quality of life. Additionally, drug treatments, such as Celoxib are recommended for FAP patients. However, some of the risk factors associated with this drug include gastrointestinal bleeding, ulceration and increased risk of stomach and intestinal perforation [100]. These effects can be fatal. Thus, elucidating molecular and cellular mechanisms underlying colorectal tumorigenesis and identification of targets that contribute to radioresistance will improve radiotherapy and help define personalized preventative treatment strategies.

Chapter II. Identification of a Tight Junction/Focal Adhesion Signaling Complex: BVES and BCAR3

Introduction

Colorectal cancer (CRC) is the second most common cause of cancer-related deaths of men and women in the United States [97]. CRC is an age-related disease that occurs with increasing incidence beginning in the 5th decade of life [83], [97]. Some of the factors associated with increased risk for developing CRC include environmental and lifestyle changes, inflammatory bowel diseases and hereditary syndromes such as hereditary nonpolyposis colorectal cancer (HNPCC) and Familial Adenomatous Polyposis (FAP) [83], [97], [101]. Development of CRC is a multifaceted process that involves a series of genetic and epigenetic changes that transform normal epithelium into malignant colorectal tumors [14], [102]. For example, mutations in Adenomatous Polyposis Coli (APC), occur at high frequency and during the early stages of the tumorigenic process [26], [103]. Functionally, APC is a negative regulator of the Wnt/β-catenin signaling pathway [19], [104], [105]. In the presence of Wnt signals, β-catenin translocates to the nucleus and complexes with TCF4. In the small intestine, the B-catenin TCF4 complex promotes Paneth cell differentiation. Paneth cells contribute to mucosal barrier function. Additionally, adherens junctions and tight junction proteins play a critical role in maintenance of barrier integrity and are mutated in colon cancer. For example, E-cadherin, an AJ molecule, can form protein complexes with B-catenin to form an epithelial barrier. Disruption of the E-cadherin/β-catenin complex can result in in cancer. Further, mutations in E-cadherin promotes increased migration, and increased tumor growth [35], [37], [106], [107]. Furthermore, nuclear

localization of Claudin-1, a tight junction protein that is critical for barrier function, has been linked to increased invasion, migration and mesenchymal acquisition of epithelial cells [33], [108]. These features are characteristics of EMT.

Interestingly, Blood Vessel Epicardial Substance (BVES), a tight junction associated protein that was discovered in screen to identify genes involved in the developing heart is downregulated via hypermethylation in colon cancer [50], [109]. Based on our studies and previous studies that site a role for junctions in cancer, we hypothesized that BVES might play a role in regulating the EMT/MET balance in colon cancer. To test this hypothesis, we restored BVES expression in LIM2405 cells and our results demonstrated BVES expression in mesenchymal-like adenocarcinoma LIM2405 cells results in the adoption of epithelial characteristics including expression of epithelial markers, trans-epithelial resistance (TER), decreased migration and invasion [38]. Then, we asked if BVES expression in SW620, a metastatic cell line that does not express BVES, would modify metastatic potential. BVES expression in SW620 cells resulted in decreased metastasis [38]. We next asked if loss of BVES expression would promote EMT in epithelial cells. To address this, we silenced BVES expression in CACO2, an epithelial-like cell line, and implanted these cells on the flanks of mice. Our results demonstrated an increased tumor burden when compared to BVES expressing CACO2 cells [38].

Mechanistically, BVES has been linked to Wnt and RhoA signaling pathways [24], [38], [58]. Through the use of yeast two-hybrid screens BVES, was shown to interact with VAMP-3, linking BVES to vesicular trafficking. BVES has

also been linked to ZO-1, coupling BVES to cell-cell interactions [48], [52]. However, the specific mechanisms are not entirely understood and the interactions with the previously tested BVES partners do not entirely explain the EMT features observed in these studies.

Given these observations, we postulated that other BVES interactors might be critical for BVES–mediated signaling events. To identify proteins that might interact with BVES, we commissioned yeast 2-hybrid screens developed by Hybrigenics (Paris, France). We identified Breast Cancer Antiestrogen Resistance-3 (BCAR3) as a BVES interacting protein. BCAR3 is a member of the novel SH2-binding protein (NSP) family of proteins, and it is the only family member that confers antiestrogen resistance [62], [64]. BCAR3, also known as SHEP1/NSP2, is a GEF that promotes formation of protrusions, increased migration and enhanced mesenchymal features in breast epithelial cells, characteristics of EMT [71], [110], [111]. Because BCAR3 was a high confidence interactor in a large-scale yeast 2-hybrid and large-scale screens are known to produce false positives, we validated the interaction via directed yeast 2-hybrid and co-immunoprecipitation. Because cell-cell contact influences BVES localization, we asked whether the BVES/BCAR3 interaction was cell density dependent. Our results demonstrated a more robust interaction under lower cell densities. To gain insight on the importance of BVES/BCAR3 function in colon cancer, we screened a previously tested panel of colon cancer cell lines for BCAR3 expression. BCAR3 expression is highest in LIM2405, a mesenchymal cell line that does not express BVES. To examine the BVES:BCAR3 relationship in this cell line,

we generated BVES inducible LIM2405 cells that stably expressed scramble or BCAR3 shRNA. Epithelial morphology was noted in the induced and noninduced cell lines but not the noninduced BVES LIM2405 cells that stably express scramble shRNA (control). Decreased migration was observed in induced and noninduced cell lines but not in control cells. Because BCAR3 promotes membrane ruffling in breast cancer cells, we asked if this finding could be extended to colon cancer cells. To answer the question, we expressed BVES in SW620 cells and noted formation of protrusions. Since protrusions are a component of cell adhesion, we postulated that the BVES:BCAR3 interaction would influence cell attachment. To examine this, we generated BVES inducible SW620 cells that stably express BCAR3 or empty vector control. We noted increases in attachment after BVES induction; however, BCAR3 had no effect on this BVES dependent phenotype.

To date, no studies have examined the role of the BVES:BCAR3 interaction in colon cancer. In this study, we have noted the phenotypic characteristics of BCAR3 expression in BVES expressing and non Bves expressing colon cancer cell lines and described BCAR3 phenotypes after genetically manipulating BCAR3 expression in BVES inducible colon cancer cell lines. BCAR3 expression in SW620 cells led to formation of protrusions, and silencing BCAR3 in non BVES induced LIM2405 cells attenuated migration. These observations support and extend what was previously reported in breast cancer cells to colon cancer cells. Furthermore, the BVES/BCAR3 interaction potentially reveals a unique tight junction to focal adhesion signaling pathway that might regulate EMT through WNT and or RhoA signaling pathways. Clarifying the role of BVES and BCAR3 in EMT may lead to

the development of more effective molecular targeting strategies to prevent colon cancer.

Materials and Methods

Yeast 2-Hybrid

An initial yeast 2-hybrid (Y2H) screen was performed by Hybrigenics (Paris, France). BVES $^{aa\ 115\text{-}360}$ was used as bait to screen against their human placental cDNA library. To validate the commissioned Y2H, we performed a directed Y2H, using yeast strain L40, provided by the Hiebert lab at Vanderbilt University.

Yeast were transformed with the carboxy terminal BVES as bait and BCAR3 as prey followed by overnight mating to generate diploids. The diploid cells contain three reporter genes: Tryptophan, Leucine, and Histidine (Trp/-Leu/-His) that are transcribed in response to bait-prey interactions. Survival of diploid yeast on -Trp/-Leu/-His media indicates an interaction. We tested for potential auto-activation by plating the bait alone. We did not observe auto-activation using this system. The BVES BCAR3 interaction was also validated in a separate directed screen using a Gal4 system. For this screen yeast strain PJ69-4A, provided by the Reynolds lab at Vanderbilt Yeast was transformed and plated as mentioned before.

Cell Lines

SW620 and LIM2405 were maintained in RPMI supplemented with 10% Fetal Bovine Serum. CACO2, HEK293T and MDCK cell lines were maintained in DMEM and supplemented with 10% FBS. All cell culture media contained 1% Penicillin/Streptomycin (Invitrogen) and 1% L-glutamine (Invitrogen). Cells were

lysed and immunoblotting was performed with anti- HA polyclonal antibody (1:1000). Morphological alterations were assessed by bright-field microscopy.

Stable cell lines

CACO2 and SW620 cells were transduced with either HA-BCAR3 or empty vector control (pHAGE6-wtCMV-HA-wtBCAR3-BrCr1-ZsGreen-W and pHAGE6-wtCMV-Empty Vector Cotnrol- DsRed gift courtesy of Dr. Adam Learner of Boston University). BCAR3 (GFP positive) expressing cells and Empty vector control (DsRed) expressing cells were flow sorted and expanded. Protein expression was analyzed by Western blot. Morphology was assessed via bright-field microscopy.

Doxycycline inducible stable cell lines

cDNA encoding BVES was recombined into pINDUCER20. LIM2405 and SW620 colon cancer cells were transduced with either pINDUCER20-Vector or pINDUCER20-BVES, selected for neomycin resistance, cultured with or without doxycycline for 48 hours and analyzed by Western blot. BVES expression was detectible between 24-48 hours after addition of doxycycline (Figure 9B).

Stable knockdown cell lines

We purchased a set of Sigma Mission shRNA lentiviral constructs targeting BCAR3 (TRCN0000072993-7) to knockdown BCAR3 and a Non-Target (scrambled) shRNA (SHC002, Sigma) was used as a control. HEK293T packaging cell line was transfected with either BCAR3 shRNA or scramble nontarget control. 48 hours later, LIM2405 cells were transduced with BCAR3 lentiviral shRNA or scramble nontarget shRNA and cultured in the presence of complete RPMI media with Puromycin. Following selection, RNA was isolated

using the Qiagen RNA Isolation Kit and cDNA was generated from 1 □g of total RNA using the iScript cDNA Synthesis Kit (Bio-Rad). Taqman qPCR was performed using BCAR3 specific probes (ABI Probe), and expression was normalized to GAPDH. Analysis was performed using the delta delta Ct method.

Co-Immunoprecipitation Assays

BCAR3 and BVES were co-overexpressed in HEK293T cells. Cells were washed 3 times with PBS and then suspended with 500 µL of cold lysis buffer. Cells were pipetted into a 1.5 mL Eppendorf tube and sonicated at setting of 2 for 2-3 seconds on ice. Sonication was repeated 10 times. Cells were centrifuged at 13,000 rpm for 10 minutes at 4°C and the supernatant was carefully transferred to another tube. 50 uL of supernatant was used for whole cell lysate (WCL). 5 uL of HA tagged magnetic beads were added to each tube containing the supernatant. Tubes were mixed by inverting and then incubated on rotating rack for 6 hours at 4°C. Tubes were placed on the magnetic rack for 30 seconds. Supernatant was removed and saved for western analysis. Beads were washed 3 times with 1 mL of ice-cold IP buffer. Magnetic beads were resuspended in 30uL of Laemmeli's sample buffer and boiled at 100°C for 5 minutes. 10 µL of sample was run on a 10% SDS PAGE.

Immunofluorescent Microscopy

MCDCK cells were grown on square coverslips to desired confluence. Cells were fixed in 70% methanol and permeabilized with 0.1% Triton X-100. Cells were blocked with BSA and incubated with BCAR3 polyclonal antibody (Bethyl) at 1:100

or BVES SBA2 antibody (gift from David Bader laboratory) at 1:250. Cells were imaged using an EVOS Fluorescent Microscope.

Cell Attachment Assay

1 X10^5 SW620 cells were seeded on 12-well tissue culture plates and treated in the presence and absence of 1mg/mL of doxycycline. Cell number was determined by hemocytometer. Cells were counted every other day over a period of 9 days. Floating cells were collected and counted by hemocytometer.

"Drill Press" Wound Assay

SW620 and LIM2405 cells were seeded on fibronectin coated 30mm dishes. Cells were serum starved overnight. Rotating drill press was used to wound the monolayer. Cells were rinsed with PBS and stimulated with 10% FBS. QCapture software was used to capture images. Wound areas were quantitated using ImageJ software. Repair of wound (restitution) was measured and calculated as follows Restitution= (initial wound area at time 0 - final wound area at 54 hours)/(initial wound measurement) *100.

Statistical Analysis

Statistical analysis was performed using GraphPad Prism software package version 5.0. The student's t test was applied to compare two groups. One-way analysis of variance (ANOVA) with Tukey's multiple comparison test to adjust for multiple tests. A value of $P<0.05$ was considered statistically significant.

Results

Identification of BCAR3 as a novel BVES interacting protein

To identify proteins interacting with BVES, a yeast two-hybrid (Y2H) screen was commissioned. The cytoplasmic portion of BVES $^{aa115-360}$ was selected as bait

to screen a human placental cDNA library. Bioinformatic analysis of the Y2H dataset yielded 26 high-probability BVES interacting proteins. The BVES interactors were analyzed and categorized by PANTHER classification system to determine proteins involved in EMT-related processes. Given these criteria, we selected Breast Cancer Antiestrogen Resistance 3 (BCAR3). BCAR3 is a GDP Exchange Factor (GEF) whose overexpression confers antiestrogen resistance (Reference). Mechanistically, BCAR3 interacts with Rho GTPases, RAC1 and CDC42 to induce changes in actin cytoskeletal and adhesion dynamics [110]. Bioinformatics and statistical analysis for BCAR3 revealed a predicted high confidence score along with a selected interaction domain (SID) (Figure 7A). Because large-scale screens generate high rates of false positives, we verified the BVES and BCAR3 interaction using two directed Y2H screens. In the first Y2H screen, we confirmed an interaction between BVES $^{\text{aa 115-360}}$ and the BCAR3 $^{\text{aa 252-600}}$ SID using a Lex A Y2H system (Figure 7B upper). In the second Y2H screen, we demonstrated an interaction between BVES $^{\text{aa 115-360}}$ and the full-length BCAR3 using a Gal4 system (Figure 7B lower), further validating that BCAR3 is a bonafide BVES partner.

A

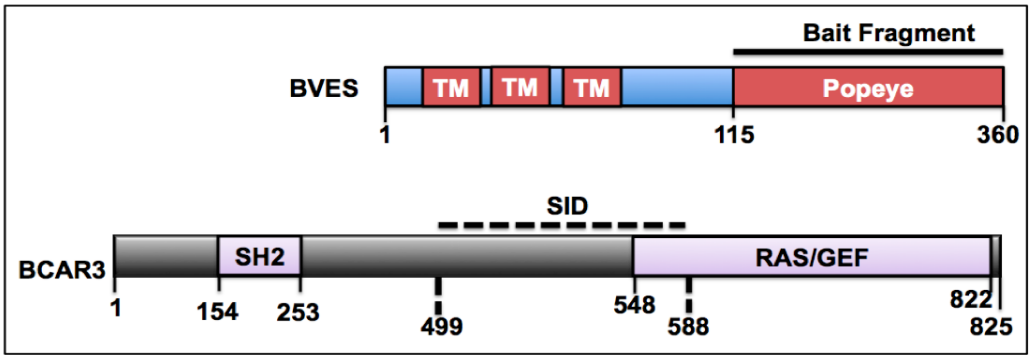

B

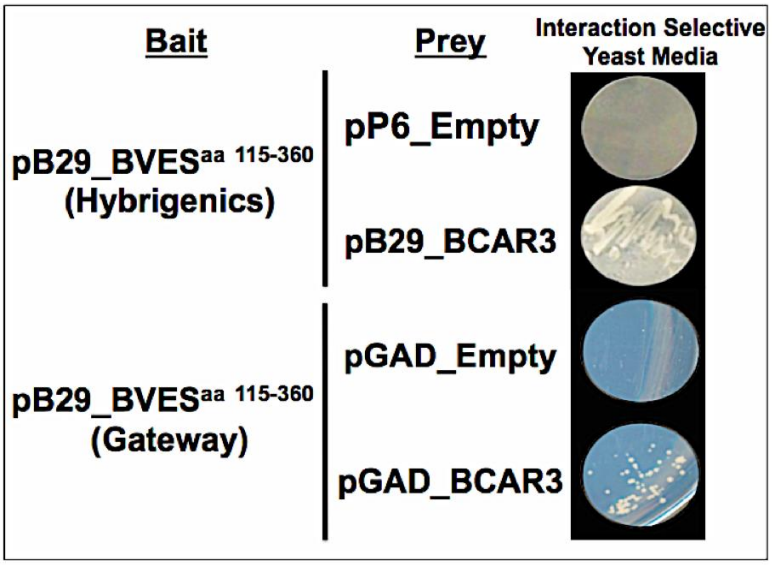

Figure 7. Y2H confirmation of BVES and BCAR3 interaction. A, Schematic diagram of labeled bait and prey constructs. Black dashed line indicate suggested interacting domain (SID) of BCAR3 that interacts with bait (BVES$^{aa115-360}$) fragment. B, Upper panel, Hybrigenics Y2H constructs. Yeast coexpressing pB29_BVES$^{aa115-360}$ as bait and pB29_BCAR3 or pB29_empty vector as prey and incubated on selective plates for 4 days. B, Lower panel, GATEWAY Y2H constructs. Yeast coexpressing pGBT9_BVES$^{aa\ 115-360}$ as bait and pGAD-BCAR3 or pGAD empty vector as prey and incubated on selective plates for 4 days.

Density dependent BVES-BCAR3 interaction

BVES subcellular distribution is influenced by cell confluence [38], [58]. For example, as cells achieve confluence, BVES localizes to the regions of cell-cell contact. To determine if BVES subcellular localization influences the interaction with BCAR3 we co-expressed V5 tagged BVES (V5-BVES) and HA tagged BCAR3 (HA-BCAR3) in HEK293T cells that were grown to 50% cell density and 100% confluence (Figure 8A). While BVES$^{aa\ 115\text{-}360}$ and full-length BCAR3 interaction was cell density independent, we observed that the full-length BVES and full-length BCAR3 interaction was more robust under sub-confluent conditions, suggesting that BVES localization influences interaction with BCAR3. These observations could mean that regions outside of the carboxy terminal may influence BVES-BCAR3 interaction.

Using Madine Darby Canine Kidney (MDCK) cells as an epithelial cell model, we evaluated endogenous association of BCAR3 and BVES via immunofluorescence double staining in MDCK cells grown to 50% and 100% cell densities. We observed BVES-BCAR3 association in MDCK cells grown to 50% confluence and not under 100% confluent conditions (Figure 8B). This data suggests that the BVES and BCAR3 association might be regulated in a density dependent fashion.

A

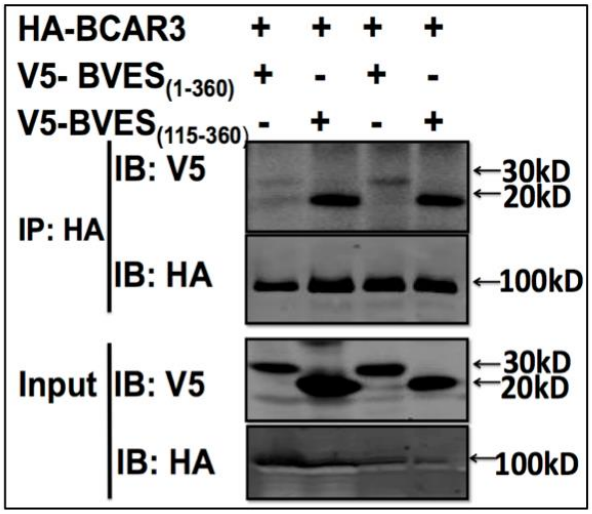

B

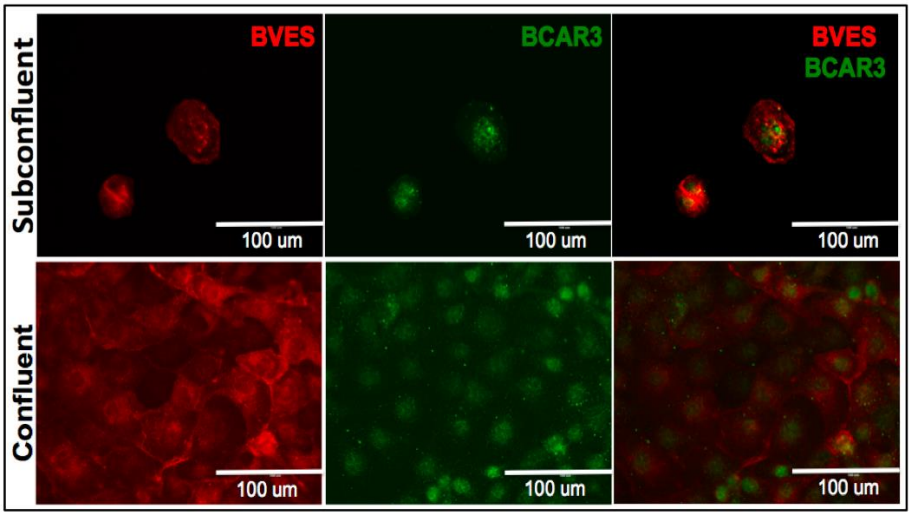

Figure 8. BVES-BCAR3 interaction depends on cell confluence. A, Co-immunoprecipitation of BVES and BCAR3 in 293T cells. Coexpression of V5 tagged BVES proteins with HA-tagged BCAR3 in 293T cells. Cells were grown to 50% or Confluent (100%) density and cell lysates were immunoprecipitated with HA antibody. Immunoprecipitants were analyzed by Western blotting with anti-HA and anti-V5 antibodies. B, Subcellular localization of endogenous BVES (Red, left panel) and BCAR3 (Green, middle panel) in MDCK cell lines grown to 50% (upper panel) or 100% (lower panel) density and visualized by immunofluorescence using anti-BVES and anti-BCAR3 antibodies. The right panels show merged images.

BVES expression affects BCAR3 expression

We had previously examined BVES dependent phenotypes in several colon cancer cell lines., we selected the CACO2, a colonic epithelial-like cell line that expresses endogenous levels of BVES and LIM2405, a mesenchymal cell line that does not express BVES to define the BVES/BCAR3 relationship. We also tested the LIM2405 and CACO2 cells for BCAR3 expression. BCAR3 levels were 8 fold higher in LIM2405 when compared to CACO2 cells (Figure 9A). Lower levels of BCAR3 in an epithelial cell line and higher in a mesenchymal cell lines, is consistent with previous reports [64]. Since BCAR3 expression is highest in the mesenchymal cell line that does not express BVES, we hypothesized that BVES expression might adversely affect BCAR3 expression. To test this hypothesis, we generated LIM2405 cells stably transduced with a lentiviral vector for the doxycycline-induced expression of BVES (p20 Inducer BVES). After induction of BVES, lysates were collected and tested for BVES and BCAR3 expression. BVES induction resulted in the loss of a single band from the characteristic doublet commonly observed for BCAR3 (Figure 9B). While it is tempting to propose that BVES might impact cleavage or post-translational modification of BCAR3, we did not test this.

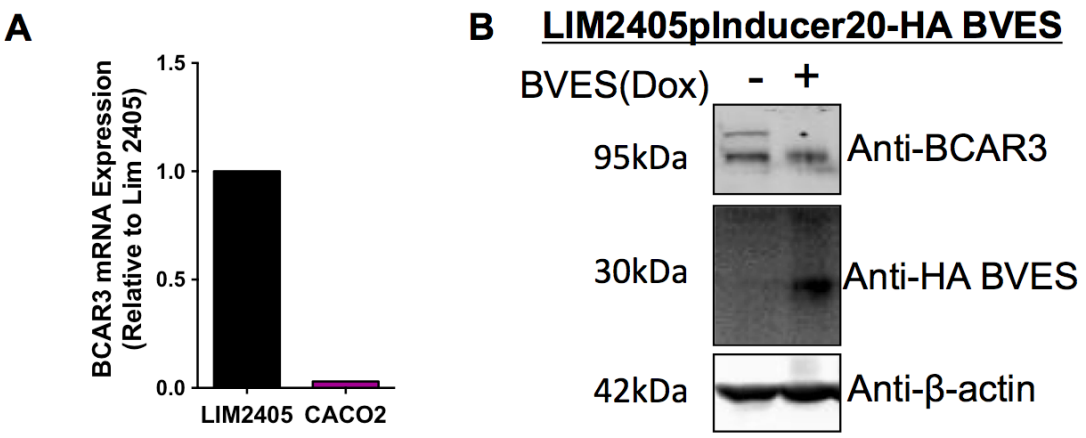

Figure 9. BVES regulates BCAR3 expression. A, qPCR for BCAR3 mRNA expression in LIM2405 and CACO2 parental cell lines. B, Western blot analysis of BVES and BCAR3 expression in BVES inducible LIM2405. Cells were either treated with doxycycline for 48 hours or untreated. Following BVES induction, cells were lysed and immunoblotted for BVES and BCAR3 using an anti-HA and anti-BCAR3 antibodies. Beta-actin was used as loading control.

BCAR3 alters cell morphology and migration in LIM2405

Because LIM2405 cells express high levels of BCAR3, we wanted to study BCAR3 function in this cell line. We generated stable BCAR3 knockdown cells by infecting LIM2405 BVES inducible cell line with BCAR3 shRNA. Stable cell lines were imaged by bright-field microscopy (Figure 10A). We observed a rounded a clustered morphology in BVES-uninduced/-induced LIM2405 cells infected with BCAR3 shRNA and BVES induced cells infected with scramble shRNA. We did not observe the clusters in BVES uninduced LIM2405 cells that were infected with scramble shRNA (Figure 10A). Based on the changes in cellular appearance, we next asked whether BCAR3 would influence migratory behavior of cells. To answer this question, we performed a “drill press” wound assay using BCAR3 knockdown cells (Figure 10B). We then waited 54 hours, the time needed for wound closure

in BVES uninduced LIM2405 cells. BVES uninduced LIM2405 infected with BCAR3 shRNA exhibited a 55% decrease in migration when compared to BVES uninduced LIM2405 infected with scramble shRNA (control cells) and BVES induced LIM2405 infected with BCAR3 shRNA reduced migratory activity by 53% when compared to control cells. While expression of BVES blunted migration by 30% in control cell line, we found no considerable differences after induction of BVES expression in the BCAR3 knockdown cells (Figure 10B). This data suggests that silencing BCAR3 expression has greater effect on colon cancer cell motility than inducing BVES. However, the lack of cellular protrusions observed in our BCAR3 knockdown cells might account for the impact of BCAR3 on migration activity.

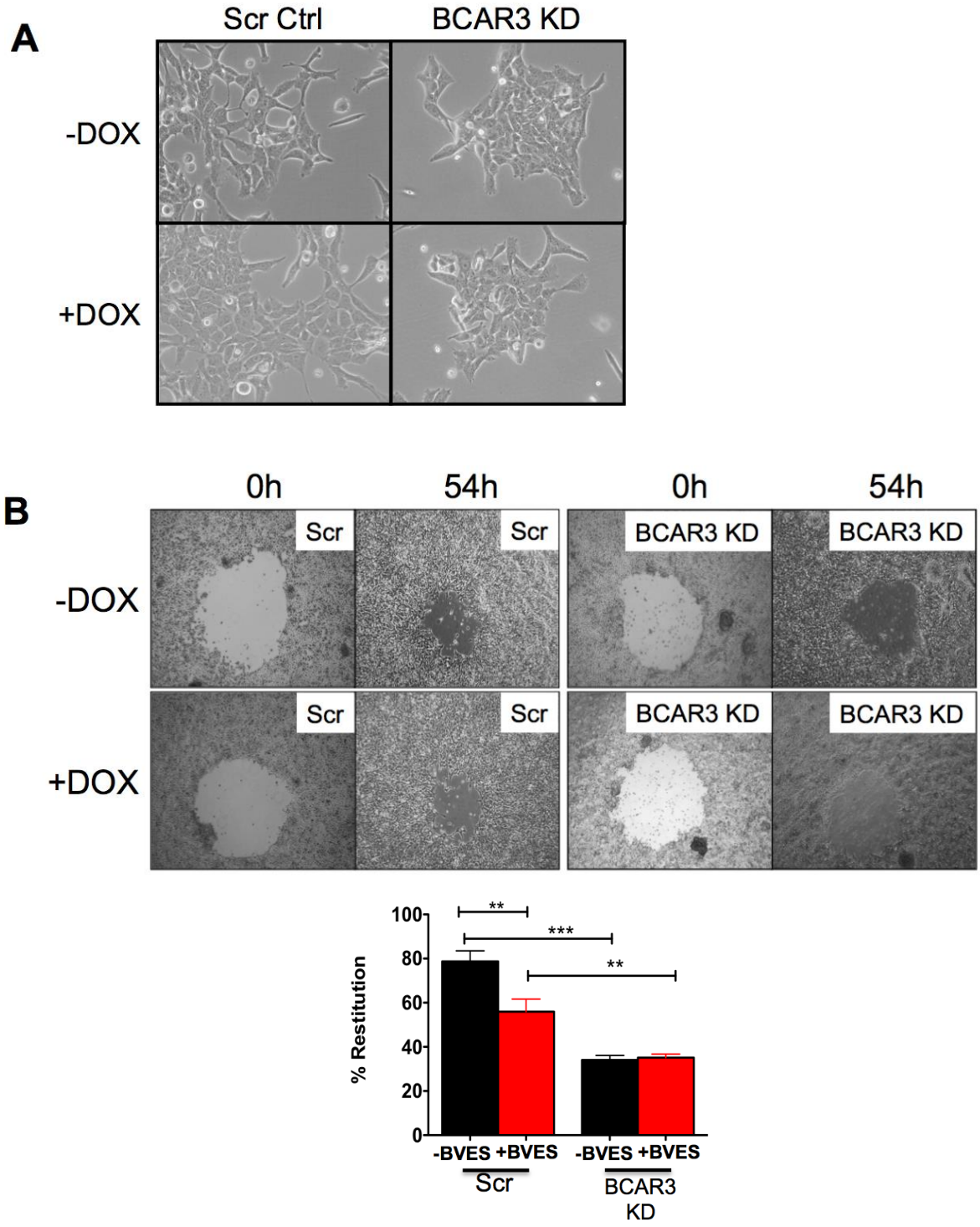

Figure 10. BCAR3 loss increases cell-cell contact and decreases cell migration. A, Bright-field microscopy image of doxycycline inducible BVES LIM2405 cells infected with scramble shRNA or BCAR3 shRNA. B, "Drill Press" Wound Assay in doxycycline inducible BVES LIM2405 cells infected with scramble shRNA or BCAR3 shRNA. Restitution, a measure of wound closure over time, was calculated as follows: % restitution=(initial wound area at time 0 - final wound area at 54 hours)/initial wound measurement) *100.

BCAR3 promotes protrusions but does not influence attachment to tissue culture substrate

Establishment of membrane protrusions is vital for cell migration and attachment [112]. Using breast cancer cell lines that display epithelial features, Rich et al have demonstrated that BCAR3 expression promotes membrane protrusiveness [111]. Given this finding and our observation that BCAR3 loss decreases migration in colon cancer cells, we hypothesize that BVES/BCAR3 interaction might influence the development of protrusions. To test this hypothesis, we overexpressed BCAR3 in CACO2 cells, an epithelial-like cell line that expresses BVES and in SW620, a mesenchymal cell line that does not express BVES. BCAR3 overexpression did not promote protrusions in CACO2 cells; however, BCAR3 expression in SW620 cells resulted in formation of membrane protrusions when compared to non-BCAR3 expressing SW620 cells (Figure 11A). Because these two cell lines possess different cellular programs and due to the lack of protrusions observed in CACO2 (BVES expressing) cells, we asked if the BCAR3/BVES relationship influenced cell attachment. To address this, we generated a BVES inducible SW620 cell line that stably expresses BCAR3 and performed daily count to determine the number of cells attached to the tissue culture surface (Figure 11B and 11C). Our results indicate that induction of BVES increases cell to surface attachment and BCAR3 has no influence on this BVES dependent phenotype (Figure 11C).

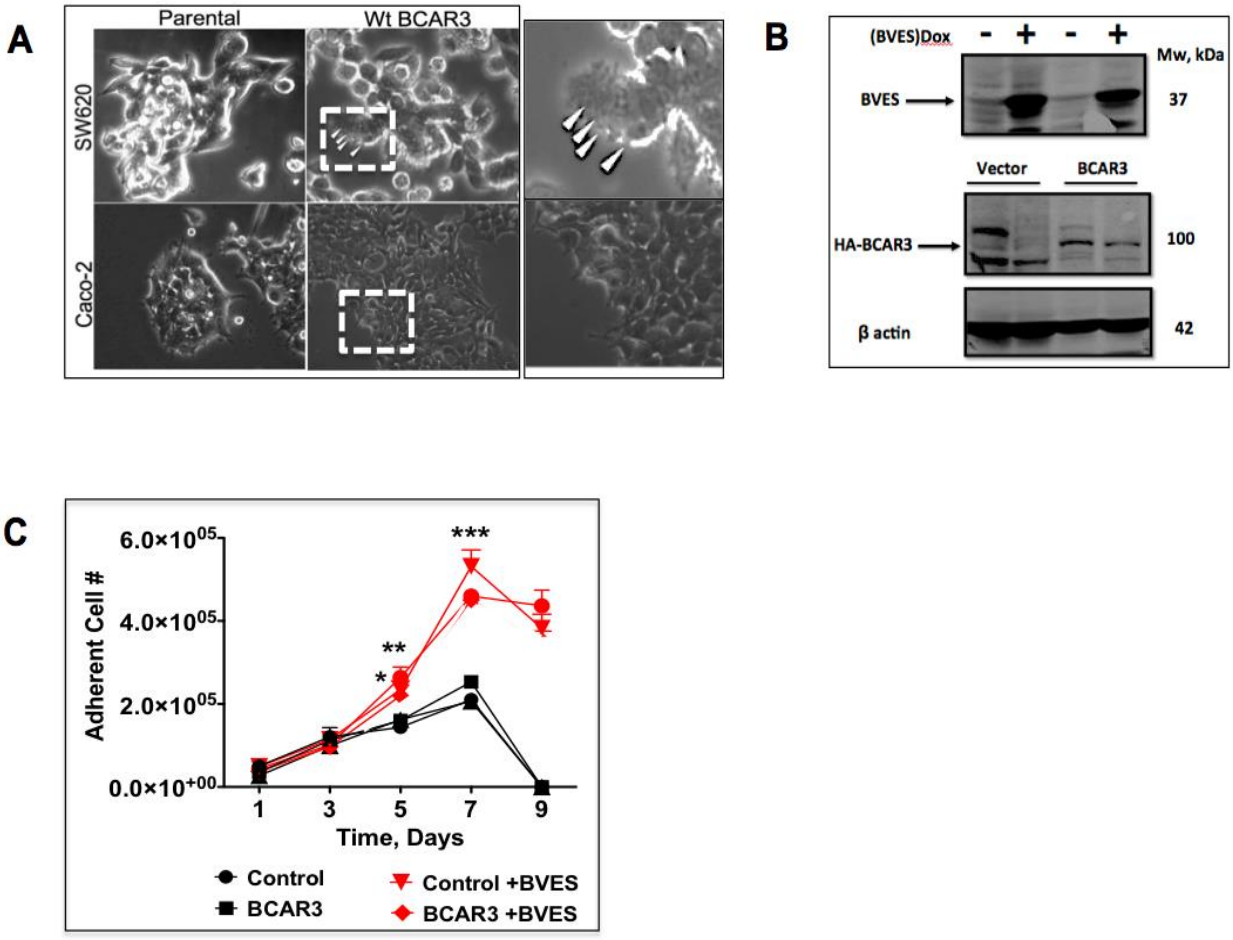

Figure 11. BCAR3 Expression promotes protrusion but does not augment BVES dependent cell attachment. A, Phase contrast microscopy demonstrating morphologic changes. White arrowheads indicate protrusions. BCAR3 expressing SW620 cells showed more cell protrusions than SW620-Vector (parental) control cells. No changes were observed in BCAR3 expressing CACO2 cells. White arrowheads indicate protrusions. B, Western blot confirming BVES inducible SW620 cell line that stably expresses BCAR3. BVES inducible SW620 cell line was transduced with WT BCAR3 or empty vector control. Cells were cultured with (+) doxycycline (DOX) or without (-) DOX for 4 days to induce BVES expression and immunoblotted with either BVES polyclonal or HA polyclonal antibody to detect BVES or BCAR3 expression, respectively. C, Cell attachment time-course assay. Induction of BVES resulted in significant increases in the number of attached cells (Control vs. BVES, $p<.05$; BCAR3 vs. BCAR3+BVES, $p<.01$).

Discussion

The objective of this study is to understand how the BVES/BCAR3 interaction modulates EMT programs in colorectal cancer cells. Previous studies have demonstrated BVES reverse EMT in colon cancer cells. However, the mechanism by which BVES transduces its signals has yet to be defined. In this study, we show that BCAR3 is a novel BVES interacting protein. Using human colon cancer cell lines, we demonstrate for the first time that loss of BCAR3 alters cellular morphology and migration in colon cancer cell lines. In reciprocal experiments, we show that BCAR3 promotes membrane protrusions.

We have previously shown that expression of BVES causes cell aggregation in non-adherent L-cells and promotes roundness in fibroblast cells [40]. Most recently, our lab has shown that BVES expression in LIM2405 cells increases expression of epithelial markers, including E-cadherin and ZO-1 and decreased expression of mesenchymal markers [38]. Not surprisingly, after BVES induction in LIM2405 we observed rounded and flat cellular appearance. Interestingly, BCAR3, a newly discovered BVES interaction promotes EMT features in breast cancer cells [62], [64], [71], [110], [113]. We observed similar epithelial–like patterning when we silenced BCAR3 in uninduced BVES LIM2405 cells and did not detect these changes in the scramble control uninduced BVES LIM2405 cells. Because Makkinje and et al have confirmed that BCAR3 associates with p130/Cas to transduce EMT signals, we hypothesized that BVES might integrate its signals to produce a BVES/BCAR3/p130Cas signaling axis. Taken together, our studies

might confirm and extend the previous findings of BCAR3 in EMT and breast cancer to colon cancer.

We have shown that BCAR3 knockdown yields a robust decrease in migration when compared to scramble control cells. Interestingly, BCAR3 knockdown in induced BVES LIM2405 cells resulted in a modest decrease in migration compared to the BCAR3 knockdown uninduced BVES LIM2405 cells. These data suggest that BCAR3 might be a downstream mediator of BVES signaling in colon cancer cells. Because inhibiting BCAR3 expression phenocopied the BVES dependent inhibitory effects on migration, we next asked whether BVES/BCAR3 interaction could influence cell adhesions. Cell attachments via cell adhesions or attachment to the surface of a tissue culture dish are indicative of properly functioning adhesions or junctions [114]. Induction of BVES in a SW620 cells resulted in increased attachment to the tissue culture surface when compared to uninduced BVES SW620 cells. Interestingly, BCAR3 expression promoted a decrease in the number of cells attaching to the dish and expression of BVES attenuated this BCAR3 mediated phenotype. Studies have shown that focal adhesion complexes are the center of regulating cell to substrate formation [67]. Because BCAR3 is able to associate with focal adhesions, the data presented might support a role for BCAR3:BVES interaction in focal adhesion assembly in colon cancer cells. Although this is speculative, this could explain how BVES induction promotes cell –substrate and -cell adhesiveness: key processes that influence migratory behavior in cells.

Furthermore, we wanted characterize the BVES/BCAR3 interaction biochemically. Immunoblotting studies demonstrated that BVES overexpression reduces endogenous levels of BCAR3 in the BVES inducible LIM2405 cells. Clearly, more work is required to understand these results but it might suggest that BVES regulates BCAR3 stability, which could ultimately influence cell adhesion.

In conclusion, we describe a role for BCAR3 in regulating key steps in EMT in colon cancer cell lines. As such, these studies could provide a major link between the tight junction and focal adhesion signaling in colon cancer. In light of this report, it is important to note that the BVES variant used for the functional studies lacked a portion of the N-terminus. At this time we do not understand the role of this domain in intracellular signaling and how this domain influences intracellular signaling including the BVES/BCAR3 signaling. Thus, our future studies will focus on mapping the critical domain that is necessary for interaction and determining whether full-length BVES impacts BCAR3 function. Importantly, understanding the BVES/BCAR3 interaction in the context of EMT and colon cancer could lead to the development of novel drug targets that would ultimately improve colon cancer therapy.

Chapter III. Transcriptional co-repressor MTG16 regulates small intestinal crypt proliferation and crypt regeneration after radiation-induced injury

Introduction

Radiation enteritis is the pathological condition whereby the mucosa becomes injured and inflamed following radiation exposure [99]. Risk factors associated with radiation enteritis include genetic mutations in DNA repair genes such as *BRCA1* and *BRCA2* [86], [87] or DNA damage response genes such as *Tp53* [88] and B-Cell Lymphoma 6 Protein (*BCL6*) [89]. Sensitivity to intestinal radiation-induced injury may be further influenced by changes in cell cycle kinetics, synchronization of replicating cell populations, or inhibition of effective DNA repair [83], [85]. Typically, DNA repair of radiation-induced DNA double-strand breaks depends on the activation of the DNA damage response that causes phosphorylation of histone H2A.X and activation of a number of mediators that phosphorylate *Tp53*. Together, the actions of these proteins ultimately lead to DNA repair, or apoptosis if DNA repair is insufficient [91].

Myeloid translocation genes (MTGs) were discovered in acute myeloid leukemia (AML) [74]. The MTGs—MTG8, MTGR1, and MTG16—serve as scaffold proteins and facilitate the formation of transcriptional repression complexes containing histone deacetylases (HDACs), nuclear receptor co-repressor 1 (NcoR) and mammalian switch-independent 3A (mSin3A) [73], [75], [115], [116]. Because MTGs are unable to bind DNA directly, association with transcription factors such as B-Cell Lymphoma 6 (BCL6), promyelocytic leukemia zinc finger (PLZF), and T-cell factor 4 (TCF4) dictate target specificity [76]. We have recently shown that MTGs compete with β-catenin for TCF4 occupancy, and MTG binding attenuates

TCF4 mediated transcriptional activation [76]. Given that TCF4 is critical for stem cell renewal in the adult intestine [117], MTGs may regulate key stem cell signaling pathways necessary for homeostasis and injury repair [73], [76]. In support of this concept, *Mtg16*$^{-/-}$ mice have stress-induced hematopoietic stem cell defects [82], as well as abnormal crypt regeneration in the colon after injury-induced inflammation [60]. However, the effect of *Mtg16* deletion on small intestine injury responses has yet to be determined.

Given that MTG16 impacts colonic responses to chemically-induced injury, we hypothesized that MTG16 may alter radiation-induced small intestinal regeneration responses. In the present study, we link MTG16 to epithelial regeneration after radiation-induced injury. At baseline, *Mtg16*$^{-/-}$ mice exhibited decreased goblet cells and higher cellular proliferation. Furthermore, after 12 Gy whole body radiation *Mtg16*$^{-/-}$ mice showed protection from radiation-induced DNA damage and p53 activation. *Ex vivo* culturing of *Mtg16*$^{-/-}$ enteroids revealed increased Wnt sensitivity and delayed maturation. Complementary to *in vivo* findings, *Mtg16*$^{-/-}$ enteroids were similarly resistant to radiation-induced death, indicating an epithelial cell-autonomous role for *Mtg16* in radiation-induced epithelial regeneration. Lastly, examination of a post-irradiation gene expression array dataset also indicated that during the proliferative recovery phase, *Mtg16* expression was reduced in stem cell populations. Taken together, results from these studies suggest that MTG16 should be explored as a potential biomarker to predict radiation sensitivity in patients.

Materials and Methods

Mouse Models

WT (C57BL/6 background) mice were obtained from Jackson Laboratories. *Mtg16*$^{-/-}$ mice were obtained from S.W. Hiebert (Vanderbilt University) and are described in detail previously [82]. *Mtg16*$^{-/-}$ and WT, both on C57BL/6 background, were used for experiments. All experiments were performed with 8 week old male and female mice. All *in vivo* experimental procedures were performed under the guidelines approved by the Vanderbilt Institutional Animal Care and Use Committee (IACUC).

Gamma Irradiation

Twenty-five 8 week old WT and *Mtg16*$^{-/-}$ mice were placed in a plexiglass-partitioning device and onto a turntable at slow speed to ensure uniform radiation dosing. Mice received 12 Gy whole body radiation from a Mark I ^{137}Cs source delivered at 1.58 Gy/min. Mice were sacrificed 4 hours after irradiation, a time known in WT mice to be associated with maximal induction of p53 mediated apoptosis [93].

To assess regenerative response, fifteen 8 week old WT and *Mtg16*$^{-/-}$ mice were dosed with 12 Gy irradiation as above and returned to their cages. 93 hours after irradiation mice were injected with 0.02 mg/kg of vincristine sulfate (Sigma-Aldrich, St. Louis, MO) to arrest cells in metaphase facilitating identification of crypt cells entering mitoses over the three hour period between administration and tissue harvest. Mice were euthanized 3 hours later (Figure 4A) at the ninety-six hour time point. The ninety-six hour post- irradiation time point was selected

because this is the time of peak proliferation of crypt stem cells and progenitors in WT mice [13], [93], [96], [118].

Immunohistochemistry and Immunofluorescence

Baseline Characterization

Following sacrifice, small intestines were removed, rinsed with Phosphate Buffered Saline (PBS), and Swiss-rolled for histological examination. The tissues were fixed in 10% formalin overnight and transferred to 70% ethanol. Tissues were submitted to the Vanderbilt University Translational Pathology Shared Resource (TPSR) core for processing and paraffin embedding. Five micron sections were cut for histology. Sections from WT and *Mtg16*$^{-/-}$ mice were evaluated for crypt morphology, crypt depth, villus height and biomarkers of secretory lineages. Goblet cells were identified by Periodic Acid-Schiff (PAS) staining. Enteroendocrine cells (EECs) were assessed by Chromogranin A (CgA) staining using anti-CgA (ImmunoStar Inc., Hudson, WI) at 1:1000. Paneth cells were identified using anti-lysozyme antibody (Dako, Carpentaria, CA) at 1:500. Proliferation was measured using anti-phospho-Histone H3 (pH3) Ser10 antibody (Millipore/Upstate Bedford, MA) that labels cells in mitotic (M) phase of cell cycle at 1:150 dilution. Vectastain Elite ABC Kit (Vector Laboratories, Burlingame, CA) was used for secondary antibody and for visualization.

Four Hours Post-Irradiation Analyses

Small intestines were harvested 4 hours post-irradiation and ~3-4 cm segments of small intestine were excised and further dissected prior to snap freezing in liquid nitrogen for use in subsequent flow cytometric analysis [119], [120]. The remaining

section of the small intestine was Swiss-rolled, fixed and submitted to the Vanderbilt TPSR core for processing and sectioning. For phospho-Histone H2A.X immunofluorescence, antigen retrieval was performed by using 500mL of 1M sodium citrate buffer (pH 6). Slides were placed in a pressure cooker and heated for 15 minutes on high pressure. Then slides were rinsed with deionized H_2O to remove excess citrate buffer. Tissue sections were permeabilized by adding 50µL of 0.1% Tween 20 to each section and allowed to incubate for 30 minutes in a covered chamber. Slides were washed twice to remove permeabilization buffer. Tissue sections were blocked in 5% goat serum in Tris-Buffered Saline (TBS). Anti-phospho-Histone H2A.X (Ser139) from Millipore (EMD Millipore, Billerica, MA) was used at 1:100 and incubated overnight at 4°C. Isotype-matched antibodies were included as negative controls. Sections were then washed in 1X PBS and incubated for one hour at room temperature in Alexa Fluor 488 goat anti-mouse-IgG (Invitrogen, Grand Island, NY) at 1:100. Slides were counterstained and mounted with ProLong Gold Antifade with 4′,6-diamidino-2-phenylindole (DAPI, Invitrogen, Grand Island, NY).

Ninety-Six Hours Post-Irradiation Analyses

At 96 hours post-irradiation, small intestines were harvested and Swiss-rolled as described above. Crypt regeneration was assessed by examination of H&E stained sections for the number of mitotic figures present per crypt. Vectastain ABC Kit was used for all immunohistochemical studies. Proliferation was measured using pH3 (see Methods: *Baseline*).

Flow Cytometric Analysis of Epithelial Cell Isolates

Frozen tissue segments were thawed in calcium and magnesium free 1X Dulbecco's Phosphate Buffered Saline (DPBS). DPBS was decanted and samples were resuspended in cold Hanks' Balanced Salt Solution (HBSS) containing 3mM ethylenediaminetetraacetic acid (EDTA) and dithiothreitol (DTT) for 1 hour with gentle shaking every 15 minutes. HBSS/EDTA/DTT solution was decanted and epithelial cells from crypt and villi were resuspended three times in 25mL of 1X DPBS. After each resuspension, conical tubes were shaken vigorously for a minimum of 30 seconds. The cell suspension was passed through a 70-µm cell strainer to remove clumps. Epithelial cells were pelleted, centrifuged at 1500 rpm for 10 min and resuspended in 1 mL of 1X DPBS. Cells were manually counted using a hemocytometer. $1x10^6$ cells were resuspended in 1 mL of 37% Formaldehyde (Ted Pella Inc., Redding, CA) diluted to a final concentration of 4% and incubated at room temperature for 10 minutes. Epithelial cell isolates were stained according to manufacturer's instructions for expression of the following antibodies: Biotinylated E-cadherin (ABCAM, Cambridge, MA) and Streptavidin-Peridinin chlorophyll protein (PerCP)-Cy5.5 tagged antibody (BD Bioscience, San Jose, CA) were used to identify epithelial cells. Phospho-Histone H2A.X (Ser139) PE conjugated antibody (Cell Signaling, USA, MA) was used to identify DNA damage in epithelial cells. The p53 antibody conjugated to Alexa Fluor 488 (Cell Signaling, Danvers, MA) was used as a marker to detect p53 induction since this is a critical mediator of radiation-induced apoptosis or DNA repair. All cells were analyzed by flow cytometry on a Becton Dickinson LSR II and first gated for E-

cadherin expression. At least 10,000 events were collected. The percentage of epithelial cells positive for phospho-Histone H2A.X or p53 was calculated using FlowJo software (TreeStar Inc., Ashland, OR).

Apoptosis Assays

Apoptosis in epithelial cell isolates was quantified using the Cell Death Detection ELISA^{PLUS} kit (Roche Applied Sciences, Indianapolis, IN) following the manufacturer's protocol. TUNEL staining on tissue sections was conducted with ApopTag Plus Peroxidase *In Situ* Apoptosis Detection Kit (EMD Millipore, Billerica, MA) according to the manufacturer's protocol. Control stains were obtained by omitting the terminal deoxynucleotide transferase (TdT) enzyme. Crypt apoptotic indices were generated by averaging the number of apoptotic cells per crypt in 40 crypts per mouse. This is presented as the mean number of TUNEL^{+} cells per crypt in each animal.

Enteroid Cultures

The crypt-enteroid culture method was modified from Shroyer *et al* [121]. Briefly, mouse proximal small intestine (~10 cm) was excised, opened longitudinally, and washed with ice-cold 1X DPBS. The intestine was cut into small pieces and incubated in ice-cold 1X DPBS containing 1mM EDTA on a rocking platform for 30 minutes. After being rinsed once with ice-cold PBS to remove EDTA, the intestinal fragments were resuspended 3 times by gentle shaking in 5mL of ice-cold 1X DPBS. After each resuspension, supernatant was collected and passed through a 70-μm cell strainer (Fisher Scientific, USA, MA) to remove villus fragments. The cell strainer was cleared using 5mL of dissociation buffer. 400 crypts were

resuspended in Matrigel (BD Bioscience) containing growth factors all obtained from R&D Systems (R&D Systems, Minneapolis, MN): 50ng/mL EGF, 100ng/mL Noggin, and 500ng/mL R-spondin (ENR media) or 100ng/mL Wnt3A+ENR (WENR media). Neither media nor growth factors were replaced throughout the course of the experiment. Plating efficiencies were calculated by dividing the total number of enterospheres formed by the original number of crypts plated at Day 0 and multiplying by 100. Enterospheres were visualized and counted at 24,48, and 72 hours after plating. Experiments were performed in duplicate and repeated three times.

Statistical Analysis

Graphs were generated using Graph Pad Prism 5.0. All data are represented as the standard deviation. Student t-test was performed to compare two groups. One-way analysis of variance with Tukey's multiple comparison tests was performed to compare more than two groups. A $P<0.05$ was considered statistically significant.

Results

*M*TG16 regulates crypt proliferation and goblet cell numbers *in vivo*

Previous studies dmonstrated that MTGs regulate lineage specification and proliferation in a variety of tissues ([81], [82] hematopoiesis; [122] colon). In the small intestine, *Mtgr1* knockout mice exhibited defects in secretory lineage allocation [80] while loss of *Mtg16* has been reported to promote colonocyte proliferation and exacerbate colonic response to injury [60]. The role of MTG16 in small intestinal biology is unknown. To define whether MTG16 deletion alters morphology, proliferation, or secretory cell lineages in small intestine, we

performed a histological characterization of *Mtg16*$^{-/-}$ mice. *Mtg16*$^{-/-}$ mice had normal crypt architecture with both villus height and crypt depth being comparable to WT mice (Figure 12A). In contrast, pH3^{+} cells/crypt-villus unit were increased in *Mtg16*$^{-/-}$ (Figure 12B) indicating increased proliferation. There were no significant differences in numbers of enteroendocrine or Paneth cells (Figure 12C). However, PAS labeled goblet cells per crypt villus unit were significantly reduced in *Mtg16*$^{-/-}$ mice (Figure 12C). Thus, MTG16 normally regulates proliferation in the small intestinal crypts and is required for efficient goblet cell production.

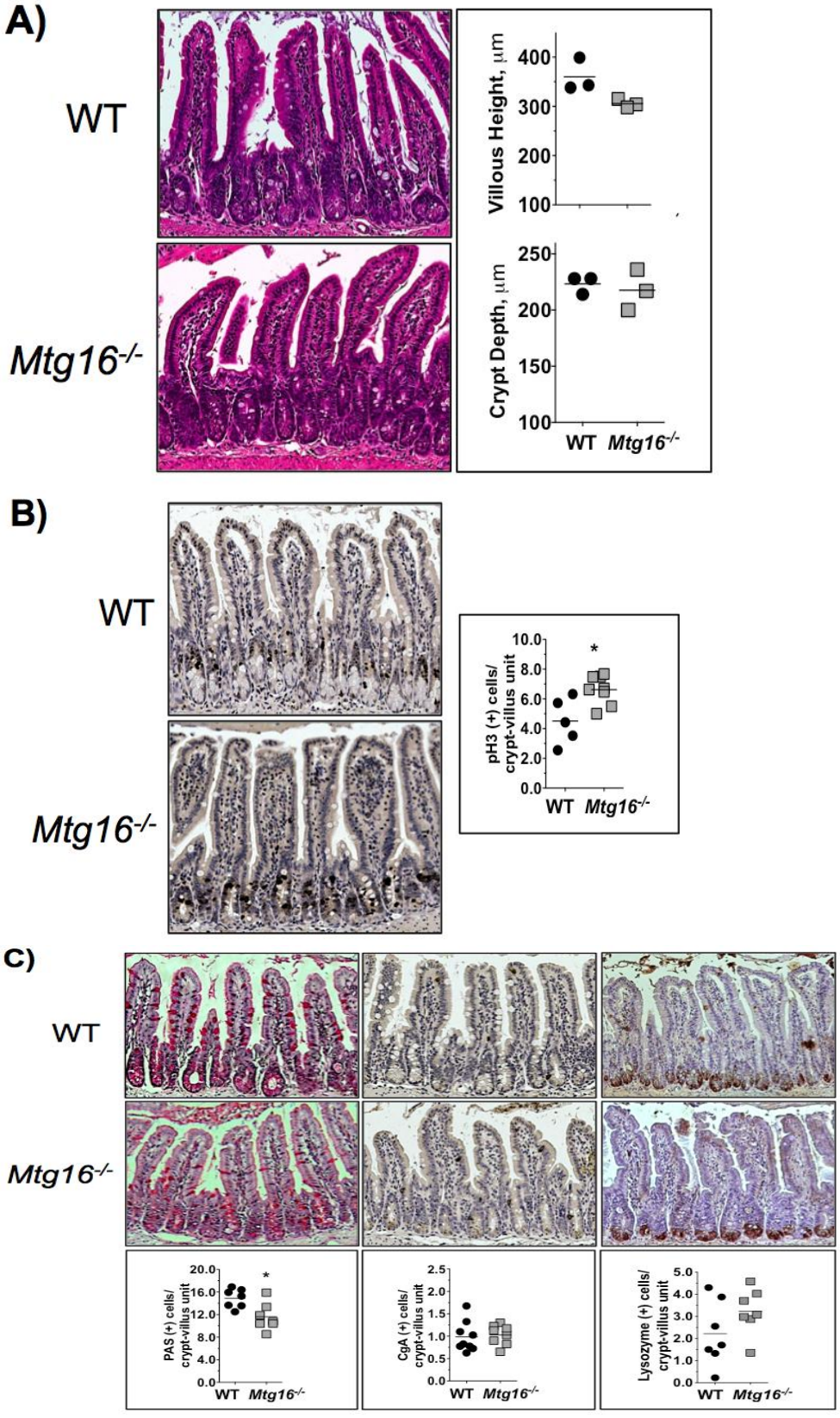
A)
WT
Mtg16-/-
Villous Height, μm
400
300
200
100
Crypt Depth, μm
250
200
150
100
WT Mtg16-/-
B)
WT
Mtg16-/-
pH3 (+) cells/ crypt-villus unit
10.0
8.0
6.0
4.0
2.0
0.0
*
WT Mtg16-/-
C)
WT
Mtg16-/-
PAS (+) cells/ crypt-villus unit
20.0
16.0
12.0
8.0
4.0
0.0
*
WT Mtg16-/-
CgA (+) cells/ crypt-villus unit
2.5
2.0
1.5
1.0
0.5
0.0
WT Mtg16-/-
Lysozyme (+) cells/ crypt-villus unit
5.0
4.0
3.0
2.0
1.0
0.0
WT Mtg16-/-

Figure 12. MTG16 regulates epithelial progenitor cell lineage allocation and proliferation. Small intestines were isolated and Swiss-rolled. A, Representative H&E demonstrating normal crypt morphology in WT and *Mtg16*$^{-/-}$ small intestine. Measurement of average villous height and crypt depth of 100 crypts from the distal small intestine demonstrating no differences between *Mtg16*$^{-/-}$ and WT mice (n=3 mice in each group). B, pH3+ cells demonstrate increased proliferation in *Mtg16*$^{-/-}$ small intestine (n=5) when compared to WT (n=8, *P=0.01). C, (i) Period Acid Schiff (PAS) stain demonstrated reduced number of goblet cells in *Mtg16*$^{-/-}$ small intestine when compared to WT (n=7 each, *P<0.05). (ii) Chromogranin A (CgA) staining demonstrated no difference in the number of enteroendocrine cells between *Mtg16*$^{-/-}$ (n=8) and WT (n=9, P=0.75). (iii) Lysozyme staining demonstrated no differences in number of Paneth cells between WT and *Mtg16*$^{-/-}$ mice (n=7 in each group, P=0.16).

MTG16 is critical for radiation-induced DNA damage response

To assess intestinal injury responses, WT and *Mtg16*$^{-/-}$ mice were exposed to 12 Gy of ionizing radiation. DNA damage and apoptosis were examined 4 hours post-irradiation (Figure 13A), the peak time for detection of p53-induced apoptosis in the small intestine [93]. Flow cytometric analysis for phospho-histone H2A.X on epithelial isolates from irradiated WT and *Mtg16*$^{-/-}$ mice revealed significantly decreased levels in *Mtg16*$^{-/-}$ intestine when compared to WT (Figure 13B). This was confirmed by immunofluorescence staining of WT and *Mtg16*$^{-/-}$ intestine for phospho-Histone H2A.X (Figure 13C). In addition, while analysis of p53 positve epithelial cells by flow cytometry revealed no significant differences between cohorts (data not shown), analysis of phospho-Histone H2A.X/p53 double positive epithelial cells by flow cytometry indicated a significant reduction in the percentage of double positive cells in epithelial isolates from *Mtg16*$^{-/-}$ mice at 4 hours post-irradiation (Figure 14A). In support of reduced DNA damage, apoptosis assessed by cell death ELISA was also reduced in *Mtg16*$^{-/-}$ intestine (Figure 14B). Taken together, these data suggest that loss of *Mtg16* reduced phospho-Histone H2A.X

levels, attenuated p53 activation, and decreased apoptosis after radiation-induced injury.

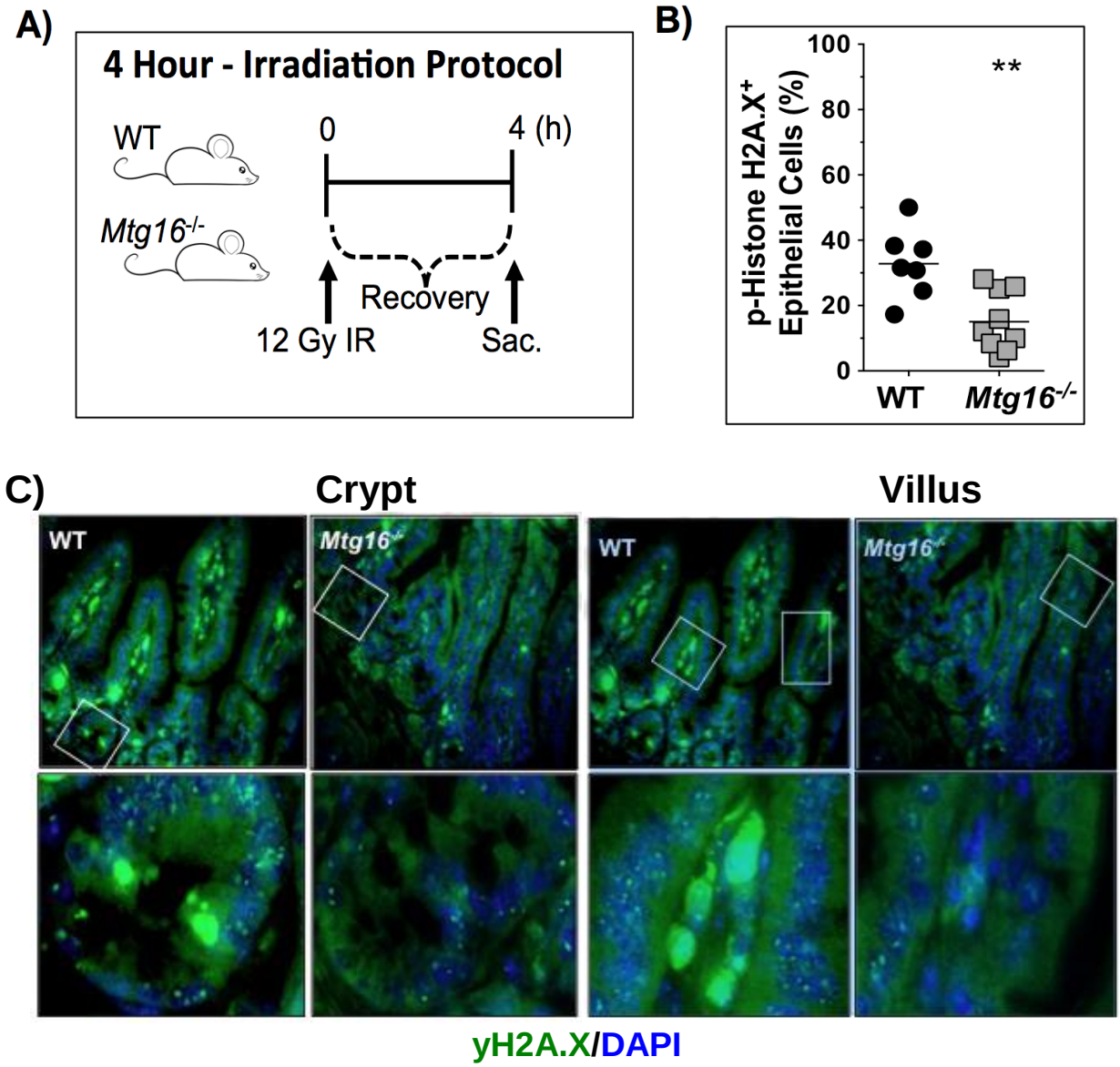

Figure 13. MTG16 is required for proper response to radiation-induced DNA damage. *A*: schematic of 4-h irradiation (IR) protocol. *B*: detection of phospho-histone H2A.X by flow cytometry in epithelial cells isolated from WT (*n*= 7) and *Mtg16*$^{-/-}$(*n* =9) mice (***P* = 0.003). *C*, *top*: representative immunofluorescent staining of WT and *Mtg16*$^{-/-}$ small intestine for phospho-*y*H2A.X with DAPI 4 h after 12 Gy irradiation (X10 magnification). The areas in white boxes are shown at higher magnification (X40 magnification) at *bottom*.

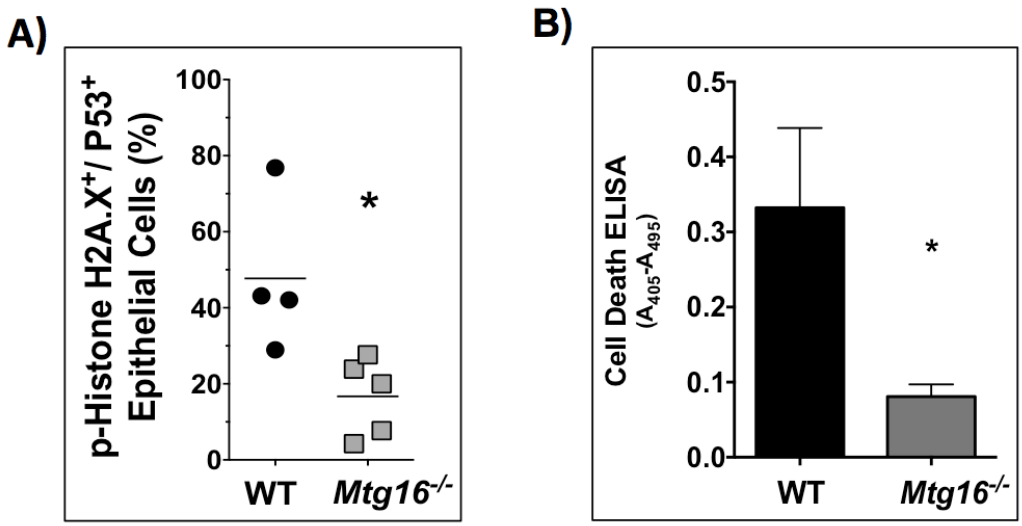

Figure 14. MTG16 is critical for p53-mediated apoptosis. A, Flow cytometry detection of phospho-Histone H2A.X and P53 in epithelial isolates from irradiated WT (n=4) and *Mtg16*$^{-/-}$ (n=5) mice (**P*=0.02). B, Apoptosis was measured by Cell Death ELISA (**P*=0.03, n=10 in each group)

MTG16 loss promotes crypt regeneration

Since we observed decreases in DNA damage and apoptosis, we postulated that MTG16 would impact crypt regenerative response [9], [90], [93] in response to ionizing radiation. Therefore, we exposed WT and *Mtg16*$^{-/-}$ mice to 12 Gy irradiation followed by a 93 hour recovery period (Figure 15A). Three hours prior to sacrifice, mice were injected with vincristine, a mitotic inhibitor. At the 96 hour time point, proliferation of stem cells leads to crypt clonogenic growth and peak crypt regeneration [13], [90], [96], [118]. *Mtg16*$^{-/-}$ mice had 20% increased crypt viability in comparison to WT mice (Figure 15B) with a concurrent reduction in TUNEL positive intestinal epithelial cells (Figure 15C). Taken together, these data indicate that the absence of MTG16 protected the epithelium from radiation-induced apoptosis.

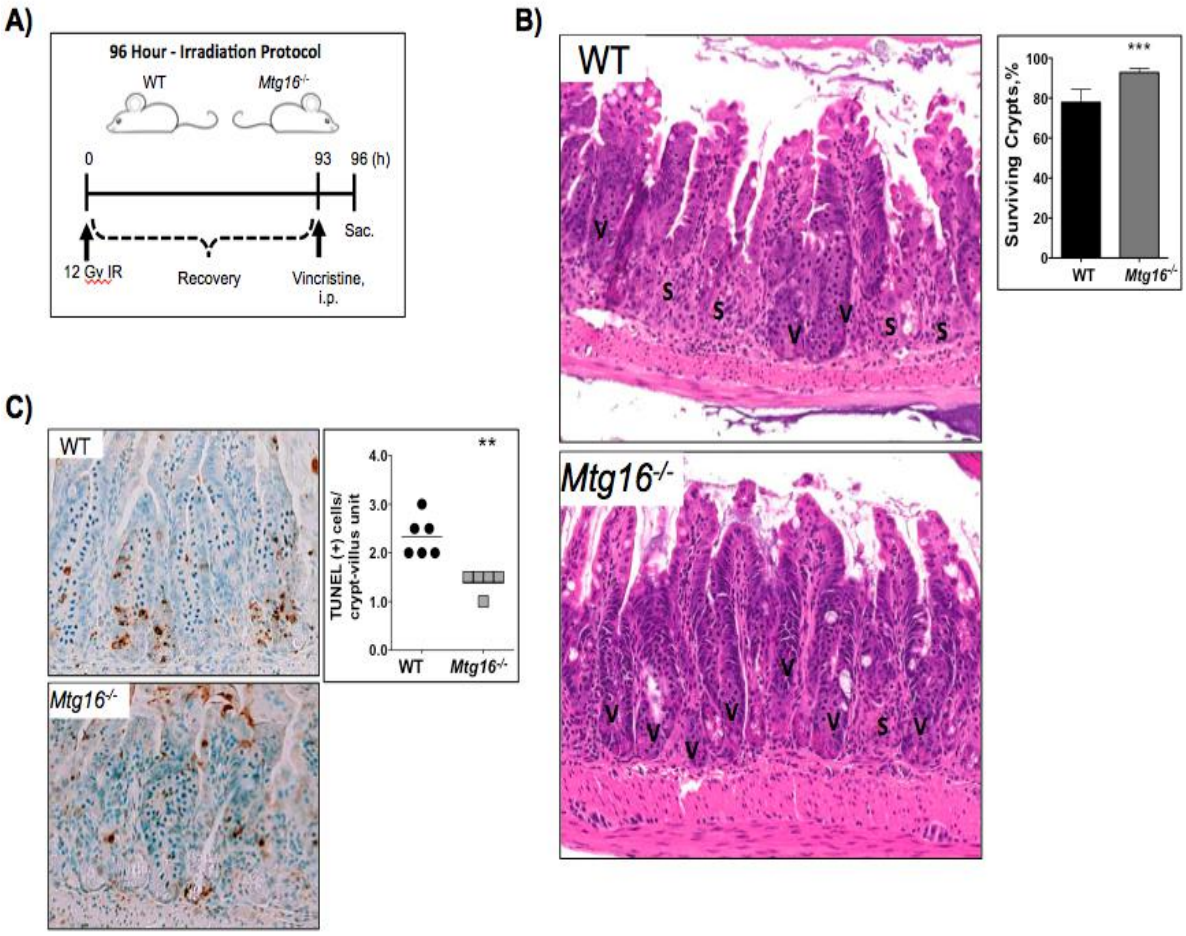

Figure 15. *Mtg16*$^{-/-}$ mice are protected from radiation-induced injury. A, Schematic diagram of 96 hour-irradiation protocol. B, Representative H&E demonstrating small intestinal crypt survival in WT and *Mtg16*$^{-/-}$ mice. The letter "V" denotes viable crypts and the letter "S" denotes sterile crypts. *Mtg16*$^{-/-}$ (n=8) mice have a higher percentage of surviving crypts than WT (n=6) (***P=0.0002). Crypts were considered viable if 3 or more mitotic bodies were observed per crypt. 40 crypts were counted per data point. The percent of surviving crypts was calculated using the following equation: (# of viable crypts/total # of crypts counted) x 100. C, TUNEL staining demonstrated a reduction in the number of TUNEL^{+} cells in *Mtg16*$^{-/-}$ (n=6) vs. WT (n=5) (**P=0.001).

MTG16 impacts stem cell growth, maturation and Wnt3A response

To investigate the mechanisms by which MTG16 might contribute to stem cell survival or growth we used enteroid cultures on crypts isolated from WT and *Mtg16*$^{-/-}$ mice. We calculated the enterospheres forming efficiency. Enterosphere

were defined as “a spherical structure composed of several small intestinal epithelial cells that appears as a rounded-off epithelial cyst” after 24 hours [123]. There were no differences in plating efficiencies between the two groups when cultured in Matrigel containing EGF, Noggin, and R-spondin (ENR) (Figure 16A). Because *Mtg16* is a negative regulator of Wnt signaling [76], we postulated that *Mtg16*$^{-/-}$ enteroids could be hyper-responsive to Wnt activation. Therefore we added Wnt3A+ENR (WENR) to the Matrigel and plated freshly isolated crypts. In Wnt3A+ENR crypt cultures, we observed a 50% higher plating efficiency in comparison to WT enteroids (Figure 16B). Interestingly, *Mtg16*$^{-/-}$ enteroids also showed reduced progression to budding enteroids compared to WT enteroids at 72 hours post plating (Figure 16C). These observations suggest that MTG16 affects stem cell growth and maturation in a Wnt-dependent manner, such that loss of *Mtg16* promotes Wnt responsiveness.

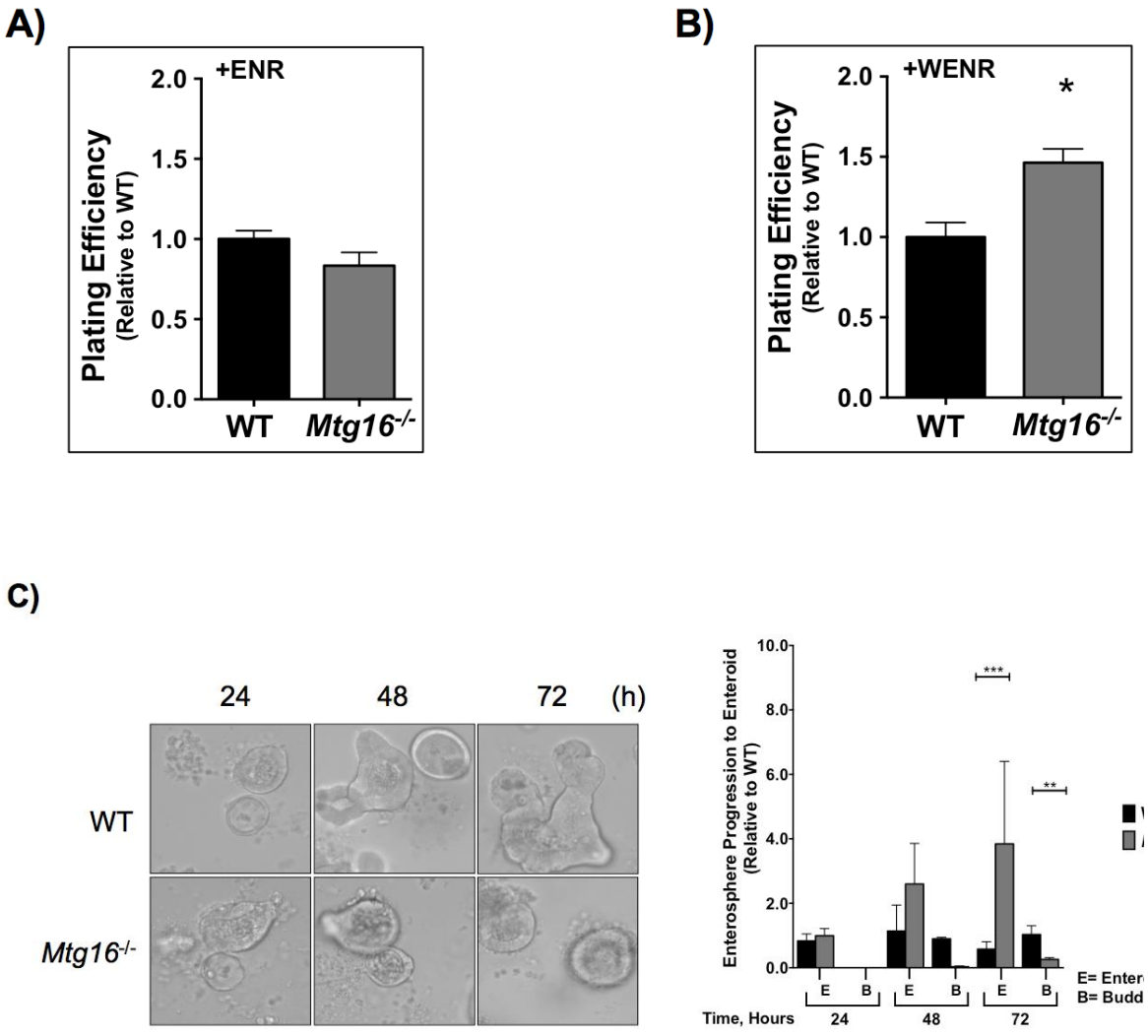

Figure 16. MTG16 regulates enteroid growth and Wnt3A response. Small intestinal crypts were isolated from WT or *Mtg16*$^{-/-}$ mice and plated at 400 crypts/well for all experiments. A, Plating efficiency was calculated for crypts embedded in Matrigel containing EGF, Noggin and R-spondin (ENR). There was no significant difference in plating efficiency between *Mtg16*$^{-/-}$ and WT intestinal crypts (*P*=0.14). Plating efficiency was calculated using the following equation: (Total # of crypts that formed enterospheres at 24 hours /total # of crypts plated at 0 hours). B, Plating efficiency was calculated for crypts embedded in Matrigel containing Wnt3A+ENR (WENR). *Mtg16*$^{-/-}$ enteroids exhibited higher plating efficiency than WT Enteroids (**P*=0.03) C, (i) Enteroid morphology at 24, 48, and 72 hours. (ii) *Mtg16*$^{-/-}$ enteroids exhibited delayed enterosphere progression to budding enteroids at 72 hours (Enterosphere: ****P*<0.0001; Budding Enteroids: ***P*<0.001) E= enterosphere and B= budding enteroid. Experiments were performed in duplicate and repeated three times.

MTG16 modulates intestinal stem cell regenerative response after irradiation

Because increased crypt regeneration was observed *in vivo* after irradiation of *Mtg16*$^{-/-}$ mice, we hypothesized that *Mtg16*$^{-/-}$ enteroid plating efficiency, a surrogate marker for stem cell survival or growth, would be similarly impacted. To test this, mice were given 12 Gy irradiation and crypts were isolated and plated in Matrigel containing ENR 4 hours later. We observed a 70% increase plating efficiency in *Mtg16*$^{-/-}$ enteroids 24 hours after plating (Figure 17A).

Given that specific gene expression programs are modified after injury and during the regenerative phase, we sought to determine if *Mtg16* was regulated in response to radiation-induced injury. Using a well-characterized Sox9 transgenic model, we assessed *Mtg16* RNA levels in different populations of Sox9-EGFP sorted cells. Prior studies demonstrated that the Wnt target gene, Sox9, is a marker for intestinal cell proliferation [96], [124]. Studies using Sox9-EGFP reporter mice demonstrated that FACS for different levels of Sox9-EGFP expression yields Sox9-EGFP^{Negative} cells enriched for enterocyte markers, Sox9-EGFP^{Sublow} enriched for progenitors, Sox9-EGFP^{Low} cells enriched for Lgr5^{+} and other intestinal stem cell markers and Sox9-EGFP^{High} cells enriched for enteroendocrine cells [96], [125]. In the present study, qRT-PCR on these populations for *Mtg16* indicated no significant difference in *Mtg16* levels across populations; however, after irradiation, *Mtg16* was specifically down-regulated in the Sox9-EGFP^{Low} stem cell enriched compartment and increased in the Sox9-EGFP^{Negative} cells (Figure 17B). Thus, these data suggest that MTG16 levels are regulated during the regenerative phase after injury.

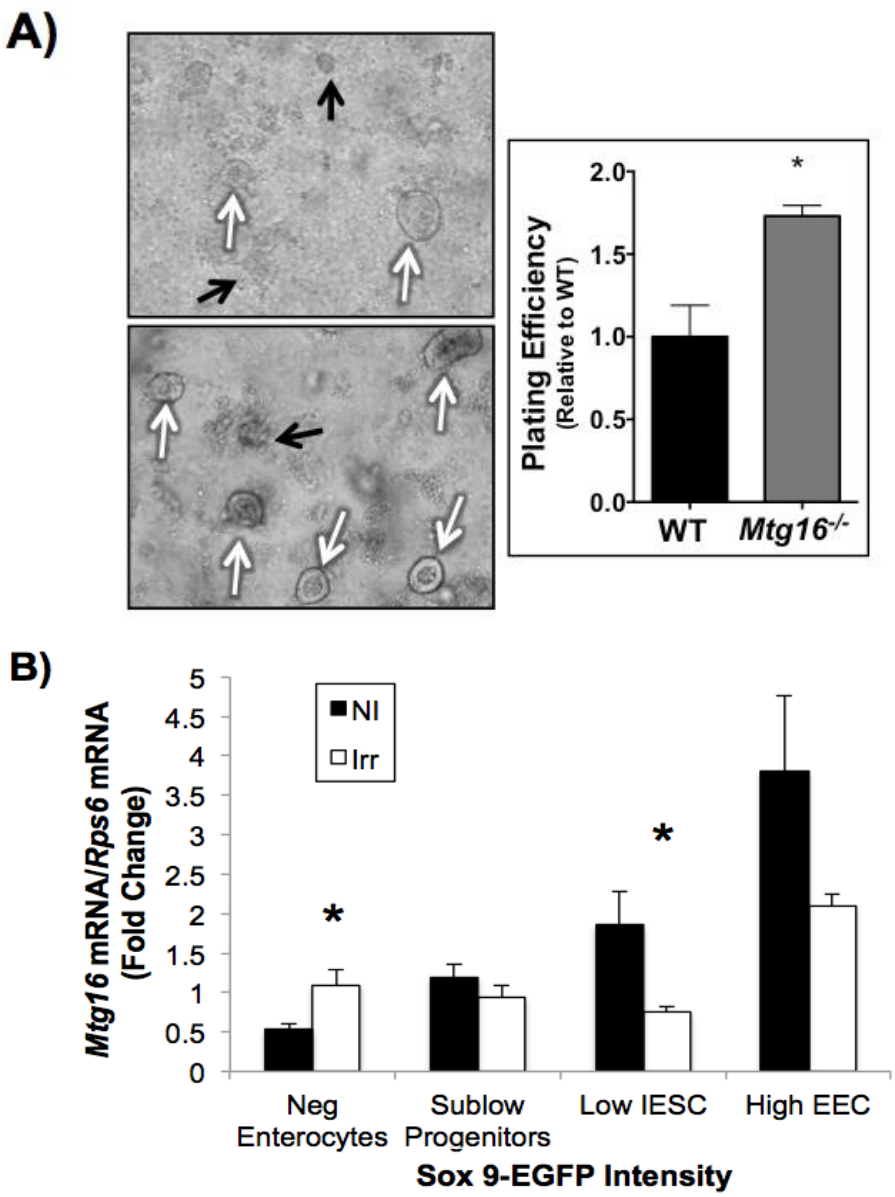

Figure 17. MTG16 decreases stem cell regenerative response after radiation-induced injury. A, Plating efficiency of intestinal crypts isolated from WT and *Mtg16*$^{-/-}$ mice dosed with 12 Gy irradiation. Higher plating efficiencies were observed in crypts isolated from Mtg16$^{-/-}$ mice when compared to crypt isolation from WT mice (*P=0.01) (White arrows indicate live and black arrows indicate dead enterospheres). Experiments were performed in duplicate and repeated three times. B, Quantitative PCR of Mtg16 expression in Sox9-EGFP^{Negative}, Sox9-EGFP^{Sublow,} Sox9-EGFP^{Low}, and Sox9-EGFP^{High} cells from the intestines of both nonirradiated and irradiated mice. No significant differences were observed in *Mtg16* mRNA levels across populations. *Mtg16* mRNA expression is lower in intestinal epithelia stem cell (IESC) enriched Sox9^{Low} and higher in terminally differentiated Sox9^{Negative} cells 5 days post-irradiation (IESCs: *P<0.05 and Enterocytes: *P<0.05, n=5 per group). Black bars represent nonirradiated (NI) and white bars represents irradiated (Irr).

Discussion

The goal of the present study was to investigate the role of MTG16 in small intestine by examining the effect of *Mtg16* deletion on baseline measurements of crypt-villus unit homeostasis and response to 12 Gy irradiation. At baseline, *Mtg16*$^{-/-}$ mice had higher cell proliferation in crypts and evidence for altered lineage allocation based on reduced PAS-stained goblet cells. *Mtg16*$^{-/-}$ enteroids were hyper-responsive to WNT activation and exhibited delayed progression to mature enteroids, suggesting altered stem cell activity in the *Mtg16*$^{-/-}$ intestine. Furthermore, after irradiation *Mtg16*$^{-/-}$ mice were protected from DNA damage and had decreased p53 activation. Additionally, *Mtg16*$^{-/-}$ crypts isolated from mice at 4 hours after 12 Gy radiation showed significant increases in plating efficiency, indicating an epithelial cell-autonomous role for MTG16 in protecting crypt stem cells from damage induced crypt death. Lastly, examination of *Mtg16* expression in isolated stem cells at the time of peak stem cell regeneration demonstrated that *Mtg16* expression was reduced in stem cell populations.

In this report, we show that *Mtg16*$^{-/-}$ mice have increased crypt proliferation at baseline indicating that MTG16 negatively regulates normal basal proliferation rate. After irradiation, and at peak time of proliferation, *Mtg16* expression is reduced in Sox9-EGFP^{Low} stem cell enriched compartments. Microarray analysis of Sox9-EGFP^{Low} stem cell has shown that genes involved in differentiation, crypt mucosal repair and radiation induced apoptosis are repressed in Sox9-EGFP^{Low} cells [96]. Given this evidence, we postulate that lower MTG16 levels might permit activation of stem cell programs promoting epithelial reconstitution. We also found

that MTG16 expression is increased in Sox9-EGFP^{Negative} population. As previously reported, by Landeghem *et. al*, Sox9-EGFP^{Negative} cells are enriched for differentiated lineages. Thus, MTG16 might limit proliferation and allow differentiation to progress in this population.

Our findings indicate that MTG16 normally plays a role in initial cellular responses to irradiation. *Mtg16*$^{-/-}$ mice have increased crypt viability, attenuated apoptosis, decreased DNA damage and decreased p53 activation. These data indicate that MTG16 normally contributes to immediate epithelial responses to irradiation. One possible explanation is perhaps MTG16 promotes activation of the DNA repair machinery. If this is the case, MTG16 loss would result in failure to recognize DNA breakage sites and phosphorylate H2A.X after radiation. Therefore, as a consequence of MTG16 deletion, *Mtg16*$^{-/-}$ mice might have DNA damage, but the initiation of the repair mechanism is defective due to reduced H2A.X phosphorylation.

Mtg16$^{-/-}$ mice exhibit hematopoietic lineage allocation defects with skewing of early myeloid progenitor cells toward granulocytic/macrophage lineages and a reduction in megakaryocyte-erythroid progenitor cells [82]. Lineage allocation differences are not limited to hematopoiesis as *Mtg16*$^{-/-}$ small intestine also has decreased goblet cell numbers. While the functional role of goblet cells in radiation injury is unclear [126]–[128], it is tempting to postulate that decreased goblet cells in *Mtg16*$^{-/-}$ mice might have impacted crypt viability after radiation injury.

The Wnt signaling pathway plays an important role in regulating intestinal epithelial stem cell function [20], [129], [130]. We have previously shown that

MTG16 competes with β-catenin for TCF4 occupancy and that in the absence of MTG16 results in increased epithelial proliferation [73], [76]. In support of enhanced TCF4 activity in response to Wnt, baseline characterization of *Mtg16*$^{-/-}$ crypts in the enteroid culture system showed increased plating efficiency and delayed maturation in the presence of Wnt3A. Furthermore, several lines of evidence support a role for WNT/β-catenin signaling in survival of stem/progenitor cell populations after radiation [124], [131]. In vivo analysis of B-galactosidase staining the TOPGAL *Mtg16* mice shows intense staining in the small intestine. *Ex vivo* studies presented here show that enteroids isolated from irradiated *Mtg16*$^{-/-}$ mice have increased survival in comparison to WT enteroids. Together, these data suggest that MTG16 may be important in modifying survival programs in stem cell populations after radiation.

Our findings indicate that MTG16 is critical for multiple aspects of small intestinal homeostasis and response to injury. Specifically, that MTG16 controls goblet cell allocation, enterocyte proliferation, and is important in radiation-induced injury responses. Some of these effects may be due to MTG16-mediated inhibition of TCF4 [73], [76] an established regulator of Wnt signaling [20]. Importantly, based on the data presented here, MTG16 could serve as a potential diagnostic marker in guiding radiotherapy. Importantly, because current treatment modalities are aimed at targeting the symptoms of radiation enteritis [132], [133], this study offers promise in understanding the underlying molecular mechanisms that regulate response to radiation therapy.

Chapter IV. Conclusions, Implications, and Future Directions

A. BVES and BCAR3 interaction in colon cancer cells

We have identified BCAR3 as a BVES interacting protein. BCAR3 appears to antagonize BVES by promoting EMT. This interaction potentially reveals a unique tight junction to focal adhesion signaling pathway important in regulating EMT. Clarifying the role of BVES and BCAR3 in EMT may lead to therapeutic strategies targeting this interaction in colon cancer. To understand the functional role of the BVES and BCAR3 interaction in this context, we applied complementary knockdown and overexpression approaches. We demonstrated loss of BCAR3 rescued BVES dependent effects on cell morphology and migration. We have confirmed that BCAR3 promotes EMT in colon cancer cells and that BVES is capable of reducing levels of BCAR3.

Current reports have shown that BCAR3 elicit signals in complex with a related family member: BCAR1/p130Cas. Disrupting this interaction will allow us to determine how BVES functions independently of BCAR3/p130Cas complexes. Near et al have established BCAR3/p130CAS uncoupling mutant, R743A and have shown that BCAR3 can elicit effects on cell adhesion and migration independent of its association with BCAR1/p130CAS [71], [72]. To determine if the EMT processes in colon cancer cells are dependent on this association it would be important to generate BCAR3R743A mutant stable cell lines. These mutant cell lines would be used to evaluate morphology, migration, and cell attachment.

Adhesion is one of the most important properties of epithelial cells. Adhesion is a measurement of the ability of cells to adhere to neighboring cells

and also a measurement of cell attachment to a substrate. In our studies we only measured cell-substrate attachment. The substrate used was an uncoated tissue culture surface. Additional studies are needed to determine if BVES/BCAR3 interaction affect the ability of cells to attach to different substrates. Additional studies are also warranted to determine the impact of BVES/BCAR3 interaction on adherence to a neighboring cell. As cell-cell contact is important for the establishment of an epithelial barrier. One way to measure the impact of BVES BCAR3 interaction on intestinal barrier would involve disrupting the interaction and measuring Transepithelial Resistance (TER).

In terms of signaling pathways, BCAR3/p130Cas complex regulates CDC42 and RAC1 activity [62]. Interestingly, BVES interacts with GEFT to reduce CDC42 and RAC1 levels [24]. CDC42 regulates cell polarity and focal adhesion turnover [134]–[136]. Importantly, mislocalization of proteins responsible for apical-basal polarity promotes tumorigenesis and cancer [137], [138]. Because BCAR3 regulates CDC42, a primary regulator of cell polarity, and BVES reduces levels of BCAR3, we hypothesize that BVES may influence cell polarity through its interaction with BCAR3. To test this hypothesis, we would generate a CACO2 BVES mimetic cell line that has a mutation that disrupts association with BCAR3. We would then perform immunofluorescence to determine localization of Syntaxin-3, an apically located protein that is required for cell polarity [139]. If Syntaxin-3 is mislocalized in the CACO2 BVES mutant cell line, this data would demonstrate a requirement for BVES/BCAR3 interaction in cell polarity. However, if Syntaxin-3

remains on the apical surface, the data would suggest that other potential BVES binding partners modify cell polarity.

As extensive works in the field of cancer biology show that mislocalization of proteins are associated with cancer. It would be important to determine if disrupting the BVES/BCAR3 interaction modulates tight junction assembly. For these studies it is important to monitor expression of junctional markers including E-cadherin and Occludin-1. As such, mislocalization would have important implications in EMT and Cancer.

Understanding the BVES/BCAR3 interaction as it relates to Rho activity will provide mechanistic insight and increase our knowledge of how BVES may regulate Rho in epithelial cells. Further analyses are needed to understand how this regulation occurs. For example, does BVES expression influence BCAR3 association with P130Cas and does BVES influence BCAR3 localization? To address these questions, BCAR3R743A stable cell line is needed to determine if BVES affects the complex or can BCAR3 signal independently of p130Cas. Additional, immunofluorescence for BCAR3 in cell lines after BVES induction would give us further insight on spatiotemporal localization of BVES and BCAR3 in colon cancer cells.

Furthermore, mapping protein-protein interaction domains is essential to understanding function. Since we have a suggested interacting domain (SID) (Figure 6) we would perform site directed mutagenesis to generate mutants lacking the SID. Then perform yeast 2-hybrid and co-immunoprecipitation assays to determine if this region is required for interaction. Once we have identified the

region necessary we would create point mutations to determine the critical site required for binding. We would then mutate this putative site and determine which sites are required to rescue the BVES dependent phenotype.

Improving colon cancer treatment strategies

In this study we show that BVES may regulate cellular BCAR3 levels. We also demonstrate that BCAR3 loss rescues BVES dependent effects on cell morphology and migration. However, the molecular mechanisms underlying these changes are not entirely understood. As both proteins have been shown to influence CDC42 and Rac1 activity, implicating a role for BVES and BCAR3 in Rho signaling pathway. Understand the nature of the BVES/BCAR3 binding interface, and the link to Rho signaling may provide further insight on how the BVES BCAR3 signaling regulates the observed phenotypes. Understanding the sites required for BVES mediated reduction in BCAR3 levels would aid in improving drug therapy strategies for colon cancer patients. Equally important, our findings suggest that previous knowledge of BCAR3 in EMT and breast cancer might be extended to further our understanding of colon cancer biology.

B. MTG16 regulates intestinal differentiation

In summary, our data provide evidence that loss of MTG16 impacts intestinal differentiation. Prior work from the Hiebert lab, demonstrated that MTGs associate with TCF4, the terminal transcription factor complex in WNT signaling, and could regulate TCF4 transcriptional activity [76]. It is possible that MTG16 regulates intestinal differentiation via repression of WNT signaling. In support of this, baseline characterization of WT and *Mtg16*$^{-/-}$ enteroids demonstrated that

Mtg16$^{-/-}$ enteroids are hypersensitive to addition of Wnt3A to the growth media and as a result *Mtg16*$^{-/-}$ enteroids exhibit higher plating efficiencies when compared to WT. Further studies, are needed to examine the transcriptional programs that are upregulated after the addition of Wnt3a to the enteroid cultures. Understanding the Wnt targets may improve our understanding of the molecular mechanisms that may contribute to the proliferative and effects on intestinal differentiation

Furthermore, changes in Wnt signaling programs may explain the differences in radiosensitivity observed between the *Mtg16*$^{-/-}$ and WT mice. To examine Wnt signaling in vivo Gupta and Fuchs developed TOPGAL mice that by measure beta galactosidase activity in the tissues along with LGR5, another target of Wnt signaling before and after irradiation. [140]. By crossing the *Mtg16*$^{-/-}$ mice to the TOPGAL reporter mice, we could assay for Beta galactosidase expression, as well as LGR5, a direct target of Wnt signaling pathway before and after exposure to irradiation. This would allow us to determine if aberrant WNT signaling contributes the radioresistance in the *Mtg16*$^{-/-}$ mice. As mentioned in the introduction, *Mtg16*$^{-/-}$ mice have early myeloid progenitor cells toward granulocytic/macrophage lineages and a reduction in megakaryocyte-erythroid progenitor cells [82]. It is possible that the hematopoietic defects would contribute to the differences in proliferation and apoptosis after irradiation of the *Mtg16*$^{-/-}$mice. To rule out if the observed differences in proliferation and apoptosis were due to hematopoietic defects, we generated intestinal epithelial organoids (enteroids) from our irradiated *Mtg16*$^{-/-}$ mice and assessed plating efficiencies. We observed higher plating efficiencies for the enteroids isolated from the irradiated *Mtg16*$^{-/-}$

mice when compared to WT enteroids. The ex vivo data supports a cell autonomous roll for MTG16 intestinal epithelial repair. Furthermore, the *Mtg16*$^{-/-}$ mouse is a global knockout mouse model. To improve up our understanding of Mtg16 in the intestinal epithelium *in vivo,* we could cross Villin-Cre mice to *Mtg16* fl/fl to obtain CreERT2; *Mtg16fl*/fl mice to restrict the loss of *Mtg16* expression to the small intestine and colonic epithelium and would allow us to better assess MTG16 mediated signaling events in the presence and absence of a stressor such as radiation injury.

MTG16 loss promotes lineage misallocation and promotes radio-resistance

While the precise role of goblet cells in radiation injury is incompletely understood, some reports suggest goblet cell number decrease and other reports demonstrate that goblet cell number increases after radiation injury [127], [141], [126]. While we demonstrated that *Mtg16*$^{-/-}$ have goblet cell lineage defect before radiation, we predict that our data might favor that the relative decrease in goblet cell number might increase crypt viability. Future studies are needed to examine goblet cell response post-irradiation. To test this, we would isolate RNA from the intestinal tissue and measure goblet cell markers by qRT-PCR. We would perform immunohistochemistry on *Mtg16*$^{-/-}$ small intestine for Muc2, alcian blue and PAS, all of which detect mucin, post-irradiation.

Notch pathway plays a critical role in cell fate specification in various tissues. When Notch is activated by DSL on the neighboring cell. This triggers a conformational change and proteolysis by gamma secretase. When the Notch intracellular domain is cleaved it translocates to the nucleus to bind CSL to trigger

transcription of Notch target genes such as Hes1. When Hes1 expression is high MATH 1 expression is low. Math1 is responsible for lineage specification to secretory cell. Expression array analysis of Notch target genes of *Mtg16*$^{-/-}$ hematopoietic progenitor cells demonstrated that Hes1 levels are significantly higher when compared to hematopoietic progenitor cells from WT mice. Notably, *Mtg16*$^{-/-}$ mice have a defect in hematopoiesis and aberrant expression of Notch target genes could explain this phenotype. More importantly, these studies highlight the importance of Notch gene expression in specification of lineages in in *Mtg16*$^{-/-}$ mice. With this in mind *Mtg16*$^{-/-}$ intestines display a defect in secretory lineage allocation. Perhaps the finding that *Mtg16*$^{-/-}$ mice have higher expression of Notch target genes, particularly increased levels of Hes1, could extend to the intestinal epithelium. Therefore, we could isolate RNA from the intestinal epithelium of *Mtg16*$^{-/-}$ mice and perform a Notch expression array to quantify expression of Notch target genes.

In our studies we show that p53/H2AX levels are lower in the *Mtg16*$^{-/-}$ post-irradiation, suggesting that loss of MTG16 shifts the cellular response away from apoptosis. When cells have been exposed to a stressor such as ionizing radiation cells universal ligand in the form of phosphatidylserine. This ligand can be detected by Annexin V. Perhaps, MTG16 could regulate phosphatidylserine and this could account for the difference in apoptosis observed post-irradiation.

MTG16 expression and patient response to therapy

Microarray data of IESCs has shown that genes involved in differentiation, crypt mucosal repair and radiation-induced apoptosis are repressed in Sox9-EGFP

Low cell [96]. Examination of this transcriptome dataset and revealed lower *Mtg16* expression in Sox9-EGFP Low intestinal stem cells and Sox9 EGFP-High EEC after irradiation suggesting that diminished expression of MTG16 may lead to a radiation-induced repair program, which may include higher cell multiplication or proliferation to compensate cell death after injury. MTG16 could be used as a predictive biomarker for patient response to radiation. To directly test this, we could obtain samples from patients that have undergone radiation and measure MTG16 levels after radiation injury. If MTG16 levels are lower in patients after radiation. The data would suggest the radiation dose given is optimal. Conversely, if MTG16 levels are higher than the cells may be more resistant to radiation therapy and dosage may need to be adjusted accordingly. Overall, these studies could lead to improved efficacy of radiotherapy.

REFERENCES

[1] "Gastrointestinal tract - New World Encyclopedia."

[2] WikipediA, "Human gastrointestinal tract," p. -, 2010.

[3] A. Vinay, K. Kapoor, and C. E. T. R, "Upper GI Tract Anatomy," *Medscape*, vol. III, pp. 8–11, 2013.

[4] A. Vinay, K. Kapoor, F. Chief, and E. Thomas, "Lower GI tract Anatomy," vol. II, p. 1899008, 2015.

[5] Kapoor, Vinay Kumar and V. K. Kapoor, "Large Intestine Anatomy," *Medscape*, 2011.

[6] J. R. Turner, "Intestinal mucosal barrier function in health and disease," *Nat Rev Immunol*, vol. 9, no. 11, pp. 799–809, Nov. 2009.

[7] Davidson College Biology Department, "Simple Columnar Epithelium," pp. 4–6, 2010.

[8] N. Barker, "Adult intestinal stem cells: critical drivers of epithelial homeostasis and regeneration," *Nat Rev Mol Cell Biol*, vol. 15, no. 1, pp. 19–33, Jan. 2014.

[9] N. Barker, M. van de Wetering, and H. Clevers, "The intestinal stem cell.," *Genes Dev.*, vol. 22, no. 14, pp. 1856–64, Jul. 2008.

[10] A. J. Carulli, L. C. Samuelson, and S. Schnell, "Unraveling intestinal stem cell behavior with models of crypt dynamics.," *Integr. Biol. (Camb).*, vol. 6, no. 3, pp. 243–57, Mar. 2014.

[11] C. Potten, A. Merritt, J. Hickman, P. Hall, and A. FARANDA, "Characterization of radiation-induced apoptosis in the small intestine and its biological implications," *Int. J. Radiat. Biol.*, vol. 65, no. 1, pp. 71–78, 1994.

[12] K. Lauber, A. Ernst, M. Orth, M. Herrmann, and C. Belka, "Dying cell clearance and its impact on the outcome of tumor radiotherapy.," *Front. Oncol.*, vol. 2, no. September, p. 116, Jan. 2012.

[13] C. S. Potten, G. Owen, D. Hewitt, C. a Chadwick, H. Hendry, B. I. Lord, and L. B. Woolford, "Stimulation and inhibition of proliferation in the small intestinal crypts of the mouse after in vivo administration of growth factors.," *Gut*, vol. 36, no. 6, pp. 864–73, Jun. 1995.

[14] E. Fearon and B. Vogelstein, “A Genetic Model for Colorectal Tumorigenesis,” *Cell*, vol. 61, pp. 759–767, 1990.

[15] H. Bouzourene, P. Chaubert, W. Seelentag, F. T. Bosman, and E. Saraga, “Aberrant crypt foci in patients with neoplastic and nonneoplastic colonic disease.,” *Hum. Pathol.*, vol. 30, no. 1, pp. 66–71, Jan. 1999.

[16] B. Shpitz, Y. Bomstein, Y. Mekori, R. Cohen, Z. Kaufman, D. Neufeld, M. Galkin, and J. Bernheim, “Aberrant crypt foci in human colons: distribution and histomorphologic characteristics.,” *Hum. Pathol.*, vol. 29, no. 5, pp. 469–75, May 1998.

[17] M. R. Nucci, C. R. Robinson, P. Longo, P. Campbell, and S. R. Hamilton, “Phenotypic and genotypic characteristics of aberrant crypt foci in human colorectal mucosa.,” *Hum. Pathol.*, vol. 28, no. 12, pp. 1396–407, Dec. 1997.

[18] R. Fodde, R. Smits, and H. Clevers, “APC, signal transduction and genetic instability in colorectal cancer.,” *Nat. Rev. Cancer*, vol. 1, no. 1, pp. 55–67, Oct. 2001.

[19] P. J. Morin, “Activation of beta -Catenin-Tcf Signaling in Colon Cancer by Mutations in beta -Catenin or APC,” *Science (80-.).*, vol. 275, no. 5307, pp. 1787–1790, Mar. 1997.

[20] T. Fevr, S. Robine, D. Louvard, and J. Huelsken, “Wnt/beta-catenin is essential for intestinal homeostasis and maintenance of intestinal stem cells.,” *Mol. Cell. Biol.*, vol. 27, no. 21, pp. 7551–9, Nov. 2007.

[21] B. Kolligs, Frank, Bommer, Guido, Goke, “Wnt/Beta-catenin/TCF signaling: A critical pathway in gastrointestinal tumrorigenesis,” *Digestion*, pp. 131–144, 2002.

[22] M. Bienz and F. Hamada, “Adenomatous polyposis coli proteins and cell adhesion.,” *Curr. Opin. Cell Biol.*, vol. 16, no. 5, pp. 528–35, Oct. 2004.

[23] J. Hülsken, W. Birchmeier, and J. Behrens, “E-cadherin and APC compete for the interaction with beta-catenin and the cytoskeleton.,” *J. Cell Biol.*, vol. 127, no. 6 Pt 2, pp. 2061–9, Dec. 1994.

[24] T. K. Smith, H. A. Hager, R. Francis, D. M. Kilkenny, C. W. Lo, and D. M. Bader, “Bves directly interacts with GEFT, and controls cell shape and movement through regulation of Rac1/Cdc42 activity.,” *Proc. Natl. Acad. Sci. U. S. A.*, vol. 105, no. 24, pp. 8298–303, Jun. 2008.

[25] I. Näthke, C. Adams, and P. Polakis, “The Adenomatous Polyposis Coli Tumor suppressor protein localizes to Plasma Membrane Sites Involved in Active Cell Migration,” *J. Cell Biol.*, vol. 134, no. 1, pp. 165–179, 1996.

[26] R. Fodde, “The APC gene in colorectal cancer.,” *Eur. J. Cancer*, vol. 38, no. 7, pp. 867–71, May 2002.

[27] “Tight Junction Proteins and Cancer.” Landes Bioscience, 2000.

[28] T. A. Martin and W. G. Jiang, “Loss of tight junction barrier function and its role in cancer metastasis.,” *Biochim. Biophys. Acta*, vol. 1788, no. 4, pp. 872–91, Apr. 2009.

[29] A. Hartsock and W. Nelson, “Adherens and Tight Junctions: Structure, Function and Connections to the Actin Cytoskeleton,” *Biochim. Biophys. Acta (BBA)- …*, vol. 1778, no. 3, pp. 660–669, 2008.

[30] M. S. Balda and K. Matter, “Tight junctions,” vol. 547, pp. 541–547, 1998.

[31] J. R. F. Caldeira, E. C. Prando, F. C. Quevedo, F. a M. Neto, C. a Rainho, and S. R. Rogatto, “CDH1 promoter hypermethylation and E-cadherin protein expression in infiltrating breast cancer.,” *BMC Cancer*, vol. 6, p. 48, Jan. 2006.

[32] A. B. Singh, A. Sharma, and P. Dhawan, “Claudin family of proteins and cancer: an overview.,” *J. Oncol.*, vol. 2010, p. 541957, Jan. 2010.

[33] P. Dhawan, A. B. Singh, N. G. Deane, Y. No, S.-R. Shiou, C. Schmidt, J. Neff, M. K. Washington, and R. D. Beauchamp, “Claudin-1 regulates cellular transformation and metastatic behavior in colon cancer.,” *J. Clin. Invest.*, vol. 115, no. 7, pp. 1765–76, Jul. 2005.

[34] P. Dhawan and A. Singh, “Claudin-1 regulates cellular transformation and metastatic behavior in colon cancer,” *J. Clin. Invest.*, vol. 115, no. 7, 2005.

[35] E. Tsanou, D. Peschos, A. Batistatou, A. Charalabopoulos, and K. Charalabopoulos, “The E-cadherin adhesion molecule and colorectal cancer. A global literature approach.,” *Anticancer Res.*, vol. 28, no. 6A, pp. 3815–26, 2008.

[36] S. Lamouille, J. Xu, and R. Derynck, “Molecular mechanisms of epithelial-mesenchymal transition.,” *Nat. Rev. Mol. Cell Biol.*, vol. 15, no. 3, pp. 178–96, Mar. 2014.

[37] C. Birchmeier, W. Birchmeier, and B. Brand-Saberi, “Epithelial-mesenchymal transitions in cancer progression.,” *Acta Anat. (Basel).*, vol. 156, no. 3, pp. 217–26, Jan. 1996.

[38] C. Williams and B. Zhang, “BVES regulates EMT in human corneal and colon cancer cells and is silenced via promoter methylation in human colorectal carcinoma,” *J. Clin. Invest.*, no. 5, 2011.

[39] D. E. Reese, M. Zavaljevski, N. L. Streiff, and D. Bader, “bves: A novel gene expressed during coronary blood vessel development.,” *Dev. Biol.*, vol. 209, no. 1, pp. 159–71, May 1999.

[40] a M. Wada, D. E. Reese, and D. M. Bader, “Bves: prototype of a new class of cell adhesion molecules expressed during coronary artery development.,” *Development*, vol. 128, no. 11, pp. 2085–93, Jun. 2001.

[41] B. Andrée, T. Hillemann, G. Kessler-Icekson, T. Schmitt-John, H. Jockusch, H. H. Arnold, and T. Brand, “Isolation and characterization of the novel popeye gene family expressed in skeletal muscle and heart.,” *Dev. Biol.*, vol. 223, no. 2, pp. 371–82, Jul. 2000.

[42] B. Andrée, A. Fleige, H.-H. Arnold, and T. Brand, “Mouse Pop1 is required for muscle regeneration in adult skeletal muscle.,” *Mol. Cell. Biol.*, vol. 22, no. 5, pp. 1504–12, Mar. 2002.

[43] D. E. Reese and D. M. Bader, “Cloning and expression of hbves, a novel and highly conserved mRNA expressed in the developing and adult heart and skeletal muscle in the human,” *Mamm. Genome*, vol. 10, no. 9, pp. 913–915, Sep. 1999.

[44] R. F. Knight, D. M. Bader, and J. R. Backstrom, “Membrane topology of Bves/Pop1A, a cell adhesion molecule that displays dynamic changes in cellular distribution during development.,” *J. Biol. Chem.*, vol. 278, no. 35, pp. 32872–9, Aug. 2003.

[45] T. K. Vasavada, J. R. DiAngelo, and M. K. Duncan, “Developmental Expression of Pop1/Bves,” *J. Histochem. Cytochem.*, vol. 52, no. 3, pp. 371–377, Mar. 2004.

[46] S. S. Breher, E. Mavridou, C. Brenneis, A. Froese, H.-H. Arnold, and T. Brand, “Popeye domain containing gene 2 (Popdc2) is a myocyte-specific differentiation marker during chick heart development.,” *Dev. Dyn.*, vol. 229, no. 3, pp. 695–702, Mar. 2004.

[47] M. Osler, T. Smith, and D. Bader, “Bves, a member of the Popeye domain-containing gene family,” *Dev. Dyn.*, vol. 235, no. 3, pp. 586–593, 2006.

[48] M. Kawaguchi, H. A. Hager, A. Wada, T. Koyama, M. S. Chang, and D. M. Bader, “Identification of a novel intracellular interaction domain essential for Bves function.,” *PLoS One*, vol. 3, no. 5, p. e2261, Jan. 2008.

[49] A. N. Ripley, M. S. Chang, and D. M. Bader, “Bves is expressed in the epithelial components of the retina, lens, and cornea.,” *Invest. Ophthalmol. Vis. Sci.*, vol. 45, no. 8, pp. 2475–83, Aug. 2004.

[50] D. Reese, M. Zavaljevski, N. Streiff, and D. Bader, “bves: A Novel Gene Expressed during Coronary Blood Vessel Development,” *Dev. Biol.*, vol. 171, pp. 159–171, 1999.

[51] M. Kawaguchi, H. a. Hager, A. Wada, T. Koyama, M. S. Chang, and D. M. Bader, “Identification of a Novel Intracellular Interaction Domain Essential for Bves Function,” *PLoS One*, vol. 3, no. 5, p. e2261, May 2008.

[52] H. A. Hager, R. J. Roberts, E. E. Cross, V. Proux-Gillardeaux, and D. M. Bader, “Identification of a novel Bves function: regulation of vesicular transport.,” *EMBO J.*, vol. 29, no. 3, pp. 532–45, Feb. 2010.

[53] S. Lin, D. Zhao, and M. Bownes, “Blood vessel/epicardial substance (bves) expression, essential for embryonic development, is down regulated by Grk/EFGR signalling.,” *Int. J. Dev. Biol.*, vol. 51, no. 1, pp. 37–44, Jan. 2007.

[54] M. E. Osler, M. S. Chang, and D. M. Bader, “Bves modulates epithelial integrity through an interaction at the tight junction.,” *J. Cell Sci.*, vol. 118, no. Pt 20, pp. 4667–78, Oct. 2005.

[55] F. M. Vega and A. J. Ridley, “Rho GTPases in cancer cell biology.,” *FEBS Lett.*, vol. 582, no. 14, pp. 2093–101, Jun. 2008.

[56] M. Bruewer, A. M. Hopkins, M. E. Hobert, A. Nusrat, and J. L. Madara, “RhoA, Rac1, and Cdc42 exert distinct effects on epithelial barrier via selective structural and biochemical modulation of junctional proteins and F-actin.,” *Am. J. Physiol. Cell Physiol.*, vol. 287, no. 2, pp. C327–35, Aug. 2004.

[57] X. Guo, L. J. Stafford, B. Bryan, C. Xia, W. Ma, X. Wu, D. Liu, Z. Songyang, and M. Liu, “A Rac/Cdc42-specific exchange factor, GEFT, induces cell proliferation, transformation, and migration.,” *J. Biol. Chem.*, vol. 278, no. 15, pp. 13207–15, Apr. 2003.

[58] P. K. Russ, C. J. Pino, C. S. Williams, D. M. Bader, F. R. Haselton, and M. S. Chang, “Bves modulates tight junction associated signaling.,” *PLoS One*, vol. 6, no. 1, p. e14563, Jan. 2011.

[59] M. Nie, S. Aijaz, I. V Leefa Chong San, M. S. Balda, and K. Matter, “The Y-box factor ZONAB/DbpA associates with GEF-H1/Lfc and mediates Rho-stimulated transcription.,” *EMBO Rep.*, vol. 10, no. 10, pp. 1125–31, Oct. 2009.

[60] C. S. Williams, A. M. Bradley, R. Chaturvedi, K. Singh, M. B. Piazuelo, X. Chen, E. M. McDonough, D. a Schwartz, C. T. Brown, M. M. Allaman, L. a Coburn, S. N. Horst, D. B. Beaulieu, Y. a Choksi, M. K. Washington, A. D. Williams, M. a Fisher, S. S. Zinkel, R. M. Peek, K. T. Wilson, and S. W. Hiebert, “MTG16 contributes to colonic epithelial integrity in experimental colitis.,” *Gut*, vol. 62, no. 10, pp. 1446–55, Oct. 2013.

[61] T. van Agthoven, T. L. van Agthoven, a Dekker, P. J. van der Spek, L. Vreede, and L. C. Dorssers, “Identification of BCAR3 by a random search for genes involved in antiestrogen resistance of human breast cancer cells.,” *EMBO J.*, vol. 17, no. 10, pp. 2799–808, May 1998.

[62] D. Cai, A. Iyer, K. N. Felekkis, R. I. Near, Z. Luo, J. Chernoff, C. Albanese, R. G. Pestell, and A. Lerner, “AND-34/BCAR3, a GDP exchange factor whose overexpression confers antiestrogen resistance, activates Rac, PAK1, and the cyclin D1 promoter.,” *Cancer Res.*, vol. 63, no. 20, pp. 6802–8, Oct. 2003.

[63] M.-L. Garron, D. Arsenieva, J. Zhong, A. B. Bloom, A. Lerner, G. M. O’Neill, and S. T. Arold, “Structural insights into the association between BCAR3 and Cas family members, an atypical complex implicated in anti-oestrogen resistance.,” *J. Mol. Biol.*, vol. 386, no. 1, pp. 190–203, Feb. 2009.

[64] R. Near and Y. Zhang, “AND34/BCAR3 differs from other NSP homologs in induction of anti□estrogen resistance, cyclin D1 promoter activation and altered breast cancer cell morphology,” *J. Cell. …*, no. January, pp. 655–665, 2007.

[65] K. Felekkis, L. a Quilliam, and A. Lerner, “Characterization of AND-34 function and signaling.,” *Methods Enzymol.*, vol. 407, no. 05, pp. 55–63, Jan. 2006.

[66] T. Nakamoto, R. Sakai, H. Honda, S. Ogawa, H. Ueno, T. Suzuki, S. Aizawa, Y. Yazaki, and H. Hirai, “Requirements for Localization of p130 cas to Focal Adhesions,” vol. 17, no. 7, pp. 3884–3897, 1997.

[67] M. Nagano, D. Hoshino, N. Koshikawa, T. Akizawa, and M. Seiki, “Turnover of focal adhesions and cancer cell migration.,” *Int. J. Cell Biol.*, vol. 2012, p. 310616, Jan. 2012.

[68] Y. Wallez, P. D. Mace, E. B. Pasquale, and S. J. Riedl, “NSP-CAS Protein Complexes: Emerging Signaling Modules in Cancer.,” *Genes Cancer*, vol. 3, no. 5–6, pp. 382–93, May 2012.

[69] N. R. Schuh, M. S. Guerrero, R. S. Schrecengost, and A. H. Bouton, “BCAR3 regulates Src/p130 Cas association, Src kinase activity, and breast cancer adhesion signaling.,” *J. Biol. Chem.*, vol. 285, no. 4, pp. 2309–17, Jan. 2010.

[70] M. R. Burnham, P. J. Bruce-Staskal, M. T. Harte, C. L. Weidow, a Ma, S. a Weed, and a H. Bouton, “Regulation of c-SRC activity and function by the adapter protein CAS.,” *Mol. Cell. Biol.*, vol. 20, no. 16, pp. 5865–78, Aug. 2000.

[71] A. Makkinje, R. I. Near, G. Infusini, P. Vanden Borre, A. Bloom, D. Cai, C. E. Costello, and A. Lerner, “AND-34/BCAR3 regulates adhesion-dependent p130Cas serine phosphorylation and breast cancer cell growth pattern.,” *Cell. Signal.*, vol. 21, no. 9, pp. 1423–35, Sep. 2009.

[72] P. Vanden Borre, R. I. Near, A. Makkinje, G. Mostoslavsky, and A. Lerner, “BCAR3/AND-34 can signal independent of complex formation with CAS family members or the presence of p130Cas.,” *Cell. Signal.*, vol. 23, no. 6, pp. 1030–40, Jun. 2011.

[73] J. N. Davis, L. McGhee, and S. Meyers, “The ETO (MTG8) gene family.,” *Gene*, vol. 303, pp. 1–10, Jan. 2003.

[74] H. Miyoshi, T. Kozu, K. Shimizu, K. Enomoto, N. Maseki, Y. Kaneko, N. Kamada, and M. Ohki, “The t(8;21) translocation in acute myeloid leukemia results in production of an AML1-MTG8 fusion transcript.,” *EMBO J.*, vol. 12, no. 7, pp. 2715–21, Jul. 1993.

[75] B. Lutterbach, J. J. Westendorf, B. Linggi, a Patten, M. Moniwa, J. R. Davie, K. D. Huynh, V. J. Bardwell, R. M. Lavinsky, M. G. Rosenfeld, C. Glass, E. Seto, and S. W. Hiebert, “ETO, a target of t(8;21) in acute leukemia, interacts with the N-CoR and mSin3 corepressors.,” *Mol. Cell. Biol.*, vol. 18, no. 12, pp. 7176–84, Dec. 1998.

[76] A. C. Moore, J. M. Amann, C. S. Williams, E. Tahinci, T. E. Farmer, J. A. Martinez, G. Yang, K. S. Luce, E. Lee, and S. W. Hiebert, “Myeloid translocation gene family members associate with T-cell factors (TCFs) and influence TCF-dependent transcription.,” *Mol. Cell. Biol.*, vol. 28, no. 3, pp. 977–87, Feb. 2008.

[77] F. Calabi and R. Pannell, “Gene Targeting Reveals a Crucial Role for MTG8 in the Gut,” vol. 21, no. 16, pp. 5658–5666, 2001.

[78] T. Sjöblom, S. Jones, L. D. Wood, D. W. Parsons, J. Lin, T. D. Barber, D. Mandelker, R. J. Leary, J. Ptak, N. Silliman, S. Szabo, P. Buckhaults, C. Farrell, P. Meeh, S. D. Markowitz, J. Willis, D. Dawson, J. K. V Willson, A. F. Gazdar, J. Hartigan, L. Wu, C. Liu, G. Parmigiani, B. H. Park, K. E. Bachman, N. Papadopoulos, B. Vogelstein, K. W. Kinzler, and V. E. Velculescu, "The consensus coding sequences of human breast and colorectal cancers.," *Science*, vol. 314, no. 5797, pp. 268–74, Oct. 2006.

[79] M. Parry, M. Rose-Zerilli, and J. Gibson, "Whole Exome Sequencing Identifies Novel Recurrently Mutated Genes in Patients with Splenic Marginal Zone Lymphoma," *PLoS One*, 2013.

[80] J. M. Amann, B. J. I. Chyla, T. C. Ellis, A. Martinez, A. C. Moore, J. L. Franklin, S. Meyers, J. E. Ohm, K. S. Luce, J. Ouelette, M. K. Washington, M. A. Thompson, S. Gautam, R. J. Coffey, R. H. Whitehead, S. W. Hiebert, L. Mcghee, A. J. Ouelette, and D. King, "Mtgr1 Is a transcriptional corepressor that is required for maintenance of the secretory cell lineage in the small intestine.," *Mol. Cell. Biol.*, 2005.

[81] S. R. Lindberg, A. Olsson, A.-M. Persson, and I. Olsson, "The Leukemia-associated ETO homologues are differently expressed during hematopoietic differentiation.," *Exp. Hematol.*, vol. 33, no. 2, pp. 189–98, Feb. 2005.

[82] B. J. Chyla, I. Moreno-Miralles, M. a Steapleton, M. A. Thompson, S. Bhaskara, M. Engel, and S. W. Hiebert, "Deletion of Mtg16, a target of t(16;21), alters hematopoietic progenitor cell proliferation and lineage allocation.," *Mol. Cell. Biol.*, vol. 28, no. 20, pp. 6234–47, Oct. 2008.

[83] A. K. Shadad, F. J. Sullivan, J. D. Martin, and L. J. Egan, "Gastrointestinal radiation injury: symptoms, risk factors and mechanisms.," *World J. Gastroenterol.*, vol. 19, no. 2, pp. 185–98, Jan. 2013.

[84] A. François, F. Milliat, O. Guipaud, and M. Benderitter, "Review Article Inflammation and Immunity in Radiation Damage to the Gut Mucosa," *Biomed Res. Int.*, vol. 2013.

[85] K. R. Brown and E. Rzucidlo, "Acute and chronic radiation injury," *J. Vasc. Surg.*, pp. 15–21, 2011.

[86] B. Nieuwenhuis, "BRCA1 and BRCA2 heterozygosity and repair of X-ray-induced DNA damage.," *Int. J. Radiat. Biol.*, vol. 78, no. 4, 2002.

[87] B. Ernestos, P. Nikolaos, G. Koulis, R. Eleni, B. Konstantinos, G. Alexandra, and K. Michael, "Increased chromosomal radiosensitivity in women carrying BRCA1/BRCA2 mutations assessed with the G2 assay.," *Int. J. Radiat. Oncol. Biol. Phys.*, vol. 76, no. 4, pp. 1199–205, Mar. 2010.

[88] D. J. Mazzatti, Y.-J. Lee, C. E. Helt, M. O'Reilly, and P. C. Keng, "p53 Modulates Radiation Sensitivity Independent of p21 Transcriptional Activation," *Am. J. Clin. Oncol.*, vol. 28, no. 1, pp. 43–50, Feb. 2005.

[89] O. Margalit, H. Amram, N. Amariglio, A. J. Simon, S. Shaklai, G. Granot, N. Minsky, A. Shimoni, A. Harmelin, D. Givol, M. Shohat, M. Oren, and G. Rechavi, "BCL6 is regulated by p53 through a response element frequently disrupted in B-cell non-Hodgkin lymphoma.," *Blood*, vol. 107, no. 4, pp. 1599–607, Feb. 2006.

[90] K. Martin, C. S. Potten, S. a Roberts, and T. B. Kirkwood, "Altered stem cell regeneration in irradiated intestinal crypts of senescent mice.," *J. Cell Sci.*, vol. 111 (Pt 1, pp. 2297–303, Aug. 1998.

[91] G. Sulli, R. Di Micco, and F. di Fagagna, "Crosstalk between chromatin state and DNA damage response in cellular senescence and cancer," *Nat. Rev. Cancer*, vol. 12, no. 10, pp. 709–20, Oct. 2012.

[92] B. Kaina, "DNA damage-triggered apoptosis: critical role of DNA repair, double-strand breaks, cell proliferation and signaling," *Biochem. Pharmacol.*, vol. 66, no. 8, pp. 1547–1554, Oct. 2003.

[93] B. J. Leibowitz, W. Qiu, H. Liu, T. Cheng, L. Zhang, and J. Yu, "Uncoupling p53 functions in radiation-induced intestinal damage via PUMA and p21.," *Mol. Cancer Res.*, vol. 9, no. 5, pp. 616–25, May 2011.

[94] W. P. Roos and B. Kaina, "DNA damage-induced cell death by apoptosis.," *Trends Mol. Med.*, vol. 12, no. 9, pp. 440–50, Sep. 2006.

[95] R. G. Bristow, S. Benchimol, and R. P. Hill, "The p53 gene as a modifier of intrinsic radiosensitivity: implications for radiotherapy.," *Radiother. Oncol.*, vol. 40, no. 3, pp. 197–223, Sep. 1996.

[96] L. Van Landeghem, M. A. Santoro, A. E. Krebs, A. T. Mah, J. J. Dehmer, A. D. Gracz, B. P. Scull, K. McNaughton, S. T. Magness, and P. K. Lund, "Activation of two distinct Sox9-EGFP-expressing intestinal stem cell populations during crypt regeneration after irradiation.," *Am. J. Physiol. Gastrointest. Liver Physiol.*, vol. 302, no. 10, pp. G1111–32, May 2012.

[97] V. S. Tammana and A. O. Laiyemo, "Colorectal cancer disparities: issues, controversies and solutions.," *World J. Gastroenterol.*, vol. 20, no. 4, pp. 869–76, Jan. 2014.

[98] F. A. Orlando, D. Tan, J. D. Baltodano, T. Khoury, J. F. Gibbs, V. J. Hassid, B. H. Ahmed, and S. J. Alrawi, "Aberrant Crypt Foci as Precursors in

Colorectal Cancer Progression," *J. Surg. Oncol.*, vol. 98, no. 3, pp. 207–213, 2008.

[99] A. H. Harb, C. Abou Fadel, and A. I. Sharara, "Radiation enteritis.," *Curr. Gastroenterol. Rep.*, vol. 16, no. 5, p. 383, May 2014.

[100] "Celebrex (Celecoxib) Drug Information: Description, User Reviews, Drug Side Effects, Interactions - Prescribing Information at RxList." [Online]. Available: http://www.rxlist.com/celebrex-drug.htm. [Accessed: 05-Aug-2014].

[101] F. Haggar and R. Boushey, "Colorectal cancer epidemiology: incidence, mortality, survival, and risk factors," *Clin. Colon Rectal Surg.*, vol. 6, no. 212, pp. 191–197, 2009.

[102] G. J. Finlay, "Genetics, molecular biology and colorectal cancer.," *Mutat. Res.*, vol. 290, no. 1, pp. 3–12, Nov. 1993.

[103] S. Powell, N. Zilz, and Y. Beazer-Barclay, "APC mutations occur early during colorectal tumorigenesis," *Nature*, 1992.

[104] R. H. Giles, J. H. van Es, and H. Clevers, "Caught up in a Wnt storm: Wnt signaling in cancer.," *Biochim. Biophys. Acta*, vol. 1653, no. 1, pp. 1–24, Jun. 2003.

[105] H. Clevers, "Wnt breakers in colon cancer.," *Cancer Cell*, vol. 5, no. 1, pp. 5–6, Jan. 2004.

[106] F. Kroepil, G. Fluegen, Z. Totikov, S. E. Baldus, C. Vay, M. Schauer, S. a Topp, J. S. A. Esch, W. T. Knoefel, and N. H. Stoecklein, "Down-regulation of CDH1 is associated with expression of SNAI1 in colorectal adenomas.," *PLoS One*, vol. 7, no. 9, p. e46665, Jan. 2012.

[107] J. Ye, D. Wu, J. Shen, P. Wu, C. Ni, J. Chen, J. Zhao, T. Zhang, X. Wang, and J. Huang, "Enrichment of colorectal cancer stem cells through epithelial-mesenchymal transition via CDH1 knockdown.," *Mol. Med. Rep.*, vol. 6, no. 3, pp. 507–12, Sep. 2012.

[108] T. A. Martin, M. D. Mason, and W. G. Jiang, "Tight junctions in cancer metastasis.," *Front. Biosci.*, vol. 16, pp. 898–936, Jan. 2011.

[109] C. S. Williams, B. Zhang, J. J. Smith, A. Jayagopal, C. W. Barrett, C. Pino, P. Russ, S. H. Presley, D. Peng, D. O. Rosenblatt, F. R. Haselton, J.-L. Yang, M. K. Washington, X. Chen, S. Eschrich, T. J. Yeatman, W. El-Rifai, R. D. Beauchamp, and M. S. Chang, "BVES regulates EMT in human corneal and colon cancer cells and is silenced via promoter methylation in

human colorectal carcinoma.," *J. Clin. Invest.*, vol. 121, no. 10, pp. 4056–69, Oct. 2011.

[110] A. L. Wilson, R. S. Schrecengost, M. S. Guerrero, K. S. Thomas, and A. H. Bouton, "Breast cancer antiestrogen resistance 3 (BCAR3) promotes cell motility by regulating actin cytoskeletal and adhesion remodeling in invasive breast cancer cells.," *PLoS One*, vol. 8, no. 6, p. e65678, Jan. 2013.

[111] R. S. Schrecengost, R. B. Riggins, K. S. Thomas, M. S. Guerrero, and A. H. Bouton, "Breast cancer antiestrogen resistance-3 expression regulates breast cancer cell migration through promotion of p130Cas membrane localization and membrane ruffling.," *Cancer Res.*, vol. 67, no. 13, pp. 6174–82, Jul. 2007.

[112] K. a DeMali and K. Burridge, "Coupling membrane protrusion and cell adhesion.," *J. Cell Sci.*, vol. 116, no. Pt 12, pp. 2389–97, Jun. 2003.

[113] R. I. Near, Y. Zhang, A. Makkinje, and P. Vanden Borre, "NIH Public Access," vol. 212, no. 3, pp. 655–665, 2009.

[114] F. Costa e Silva Filho and G. Conde Menezes, "Osteoblasts attachment and adhesion: how bone cells fit fibronectin-coated surfaces," *Mater. Sci. Eng. C*, vol. 24, no. 5, pp. 637–641, Nov. 2004.

[115] L. J. Wang J, Hoshino T, Redner RL, Kajigaya S, "ETO , fusion partner in t (8 ; 21) acute myeloid leukemia , represses transcription by interaction with the human," *Proc. Natl. Acad. Sci. U. S. A.*, vol. 95, no. September, pp. 10860–10865, 1998.

[116] J. M. Amann, J. Nip, D. K. Strom, B. Lutterbach, H. Harada, N. Lenny, J. R. Downing, S. Meyers, and S. W. Hiebert, "ETO , a target of t (8 ; 21) in acute Leukemia , makes distinct contacts with multiple histone deacetylases and binds mSin3A through Its oligomerization domain.," *Mol. Cell. Biol.*, vol. 21, no. 19, pp. 6470–6483, 2001.

[117] J. H. van Es, A. Haegebarth, P. Kujala, S. Itzkovitz, B.-K. Koo, S. F. Boj, J. Korving, M. van den Born, A. van Oudenaarden, S. Robine, and H. Clevers, "A critical role for the Wnt effector Tcf4 in adult intestinal homeostatic self-renewal.," *Mol. Cell. Biol.*, vol. 32, no. 10, pp. 1918–27, May 2012.

[118] C. S. Potten and C. a Chadwick, "Small intestinal growth regulatory factors extracted by simple diffusion from intact irradiated intestine and tested in vivo.," *Growth Factors*, vol. 10, no. 1, pp. 63–75, Jan. 1994.

[119] R. Chaturvedi, M. Asim, and J. Romero–Gallo, “Spermine Oxidase mediates the gastric cancer risk associated with Helicobacter pylori CagA.,” *Gastroenterology*, vol. 141, no. 5, pp. 1696–1708, 2011.

[120] R. Chaturvedi, M. Asim, M. B. Piazuelo, F. Yan, D. P. Barry, J. C. Sierra, A. G. Delgado, S. Hill, R. a Casero, L. E. Bravo, R. L. Dominguez, P. Correa, D. B. Polk, M. K. Washington, K. L. Rose, K. L. Schey, D. R. Morgan, R. M. Peek, and K. T. Wilson, “Activation of EGFR and ERBB2 by Helicobacter pylori results in survival of gastric epithelial cells with DNA damage.,” *Gastroenterology*, vol. 146, no. 7, pp. 1739–1751.e14, Jun. 2014.

[121] M. M. Mahe, E. Aihara, M. A. Schumacher, Y. Zavros, M. H. Montrose, M. A. Helmrath, T. Sato, and N. F. Shroyer, “Establishment of Gastrointestinal Epithelial Organoids,” vol. 3, no. December, pp. 217–240, 2013.

[122] C. S. Williams, A. M. Bradley, R. Chaturvedi, K. Singh, M. B. Piazuelo, X. Chen, E. M. McDonough, D. a Schwartz, C. T. Brown, M. M. Allaman, L. a Coburn, S. N. Horst, D. B. Beaulieu, Y. a Choksi, M. K. Washington, A. D. Williams, M. a Fisher, S. S. Zinkel, R. M. Peek, K. T. Wilson, and S. W. Hiebert, “MTG16 contributes to colonic epithelial integrity in experimental colitis.,” *Gut*, no. 10, pp. 1446–55, Oct. 2013.

[123] M. Stelzner, M. Helmrath, J. C. Y. Dunn, S. J. Henning, C. W. Houchen, C. Kuo, J. Lynch, L. Li, S. T. Magness, M. G. Martin, M. H. Wong, and J. Yu, “A nomenclature for intestinal in vitro cultures.,” *Am. J. Physiol. Gastrointest. Liver Physiol.*, vol. 302, no. 12, pp. G1359–63, Jun. 2012.

[124] Y. Kim, K. H. Kim, J. Lee, Y.-A. Lee, M. Kim, S. J. Lee, K. Park, H. Yang, J. Jin, K. M. Joo, J. Lee, and D.-H. Nam, “Wnt activation is implicated in glioblastoma radioresistance.,” *Lab. Invest.*, vol. 92, no. 3, pp. 466–73, Mar. 2012.

[125] K. S. Yan, L. A. Chia, X. Li, A. Ootani, J. Su, J. Y. Lee, N. Su, Y. Luo, S. C. Heilshorn, M. R. Amieva, E. Sangiorgi, M. R. Capecchi, and C. J. Kuo, “The intestinal stem cell markers Bmi1 and Lgr5 identify two functionally distinct populations.,” *Proc. Natl. Acad. Sci. U. S. A.*, pp. 1–6, 2012.

[126] J. M. van Dongen, J. Kooyman, and W. J. Visser, “The influence of 400 r x-irradiation on the number and the localization of mature and immature goblet cells and Paneth cells in intestinal crypt and villus.,” *Cell Tissue Kinet.*, vol. 9, pp. 65–75, 1976.

[127] A. Becciolini and D. Fabbrica, “Quantitative changes in the goblet cells of the rat small intestine after radiation.,” *Acta radiol.*, vol. 24, no. October 1984, 1985.

[128] M. Kanter and M. Akpolat, “Vitamin C protects against ionizing radiation damage to goblet cells of the ileum in rats.,” *Acta Histochem.*, vol. 110, no. 6, pp. 481–90, Jan. 2008.

[129] D. Pinto, A. Gregorieff, H. Begthel, and H. Clevers, “Canonical Wnt signals are essential for homeostasis of the intestinal epithelium,” pp. 1709–1713, 2003.

[130] A. Gregorieff and H. Clevers, “Wnt signaling in the intestinal epithelium: from endoderm to cancer.,” *Genes Dev.*, vol. 19, no. 8, pp. 877–90, Apr. 2005.

[131] W. a Woodward, M. S. Chen, F. Behbod, M. P. Alfaro, T. a Buchholz, and J. M. Rosen, “WNT/beta-catenin mediates radiation resistance of mouse mammary progenitor cells.,” *Proc. Natl. Acad. Sci. U. S. A.*, vol. 104, no. 2, pp. 618–23, Jan. 2007.

[132] N. D. Carr and D. Holden, “Pathogenesis and treatment of radiation bowel disease: Discussion Paper.,” *J. R. Soc. Med.*, pp. 1–4, 1986.

[133] J. Schembri, M. Azzopardi, and P. Ellul, “Small bowel radiation enteritis diagnosed by capsule endoscopy.,” *BMJ Case Rep.*, vol. 2014, pp. 2013–2014, Jan. 2014.

[134] S. Etienne-Manneville and A. Hall, “Cdc42 regulates GSK-3β and adenomatous polyposis coli to control cell polarity,” *Nature*, vol. 421, no. February, pp. 753–756, 2003.

[135] S. Etienne-Manneville, “Cdc42--the centre of polarity.,” *J. Cell Sci.*, vol. 117, no. Pt 8, pp. 1291–300, Mar. 2004.

[136] N. Osmani, F. Peglion, P. Chavrier, and S. Etienne-Manneville, “Cdc42 localization and cell polarity depend on membrane traffic.,” *J. Cell Biol.*, vol. 191, no. 7, pp. 1261–9, Dec. 2010.

[137] M. E. Feigin, S. D. Akshinthala, K. Araki, A. Z. Rosenberg, L. B. Muthuswamy, B. Martin, B. D. Lehmann, H. K. Berman, J. a Pietenpol, R. D. Cardiff, and S. K. Muthuswamy, “Mislocalization of the cell polarity protein scribble promotes mammary tumorigenesis and is associated with basal breast cancer.,” *Cancer Res.*, vol. 74, no. 11, pp. 3180–94, Jun. 2014.

[138] L. Zhan, A. Rosenberg, K. C. Bergami, M. Yu, Z. Xuan, A. B. Jaffe, C. Allred, and S. K. Muthuswamy, “Deregulation of scribble promotes mammary tumorigenesis and reveals a role for cell polarity in carcinoma.,” *Cell*, vol. 135, no. 5, pp. 865–78, Nov. 2008.

[139] N. Sharma, S. H. Low, S. Misra, B. Pallavi, and T. Weimbs, “Apical targeting of syntaxin 3 is essential for epithelial cell polarity.,” *J. Cell Biol.*, vol. 173, no. 6, pp. 937–48, Jun. 2006.

[140] R. DasGupta and E. Fuchs, “Multiple roles for activated LEF/TCF transcription complexes during hair follicle development and differentiation.,” *Development*, vol. 126, no. 20, pp. 4557–68, Oct. 1999.

[141] K. Carr and A. Nelson, “Characterization through a data display of the different cellular responses in X-irradiated small intestine.,” *J. Radiat. Res.*, 1992.

[142] N. Barker, S. Bartfeld, and H. Clevers, “Tissue-resident adult stem cell populations of rapidly self-renewing organs.,” *Cell Stem Cell*, vol. 7, no. 6, pp. 656–70, Dec. 2010.

[143] H. J. Maier, T. Wirth, and H. Beug, “Epithelial-mesenchymal transition in pancreatic carcinoma.,” *Cancers (Basel).*, vol. 2, no. 4, pp. 2058–83, Jan. 2010.